USGS
science for a changing world

Prepared in cooperation with the Mid-Ohio Regional Planning Commission;
the Ohio Water Development Authority; the City of Columbus, Ohio; and Del-Co Water Company

Hydrologic Effects of Potential Changes in Climate, Water Use, and Land Cover in the Upper Scioto River Basin, Ohio

Scientific Investigations Report 2015–5024

U.S. Department of the Interior
U.S. Geological Survey

Cover. O'Shaughnessy Dam on the Scioto River near Dublin, Ohio. (Rendering based on original photograph by Chad Toussant, U.S. Geological Survey.)

Hydrologic Effects of Potential Changes in Climate, Water Use, and Land Cover in the Upper Scioto River Basin, Ohio

By Andrew Ebner, G.F. Koltun, and Chad J. Ostheimer

Prepared in cooperation with the Mid-Ohio Regional Planning Commission;
the Ohio Water Development Authority; the City of Columbus, Ohio;
and Del-Co Water Company

Scientific Investigations Report 2015–5024

U.S. Department of the Interior
U.S. Geological Survey

U.S. Department of the Interior
SALLY JEWELL, Secretary

U.S. Geological Survey
Suzette M. Kimball, Acting Director

U.S. Geological Survey, Reston, Virginia: 2015

For more information on the USGS—the Federal source for science about the Earth, its natural and living resources, natural hazards, and the environment—visit http://www.usgs.gov or call 1–888–ASK–USGS.

For an overview of USGS information products, including maps, imagery, and publications, visit http://www.usgs.gov/pubprod/.

Suggested citation:
Ebner, Andrew, Koltun, G.F., and Ostheimer, C.J., 2015, Hydrologic effects of potential changes in climate, water use, and land cover in the Upper Scioto River Basin, Ohio: U.S. Geological Survey Scientific Investigations Report 2015–5024, 34 p., 7 app., http://dx.doi.org/10.3133/sir20155024.

ISSN 2328-0328 (online)

Contents

Figures

Figures—continued

Figures—continued

Tables

Appendixes

[Each appendix may be downloaded as a separate file at http://dx.doi.org/10.3133/sir20155024]

Conversion Factors

[Inch/Pound to International System of Units[

Multiply	By	To obtain
	Length	
foot (ft)	0.3048	meter (m)
	Area	
acre	0.004047	square kilometer (km^2)
square mile (mi^2)	259.0	hectare (ha)
square mile (mi^2)	2.590	square kilometer (km^2)
	Volume	
million gallons (Mgal)	3,785	cubic meter (m^3)
	Flow rate	
cubic foot per second (ft^3/s)	0.02832	cubic meter per second (m^3/s)
million gallons per day (Mgal/d)	0.04381	cubic meter per second (m^3/s)
	Mass	
ton, short	9.0718E−10	Gigatonne (Gt)

Abbreviations

BCSD	Bias-corrected spatially downscaled
CDF	Cumulative distribution function
GCM	Global climate model
CMIP3	Coupled Model Intercomparison Project - Phase 3
GHG	Greenhouse gas
GIS	Geographic information system
HSPF	Hydrologic Simulation Program—FORTRAN
IPCC	Intergovernmental Panel on Climate Change
MORPC	Mid-Ohio Regional Planning Commission
MWCD	Muskingum Watershed Conservancy District
NGVD 29	National Geodetic Vertical Datum of 1929
ODNR	Ohio Department of Natural Resources
PCMDI	Program for Climate Model Diagnosis and Intercomparison
SAS	Statistical Analysis System
SRES	Special Report on Emissions Scenarios
USACE	U.S. Army Corps of Engineers
USGS	U.S. Geological Survey
WRCP	World Climate Research Programme
WGCM	Working Group on Coupled Modelling
WWFRP	Water Withdrawal Facilities Registration Program

Acknowledgments

The authors acknowledge the general help and guidance of the Sustaining Scioto Steering Committee and thank William Coon (U.S. Geological Survey) for his assistance with researching and codifying the reservoir operations. We also thank AQUA TERRA Consultants for their assistance and advice regarding HSPF-related software and the many individuals and agencies that provided information and data on water uses and reservoir operations used to construct the model. Finally, we acknowledge the Program for Climate Model Diagnosis and Intercomparison (PCMDI) and the World Climate Research Programme (WCRP) Working Group on Coupled Modelling (WGCM) for their roles in making available the WCRP CMIP3 datasets. Support for that effort was provided by the Office of Science, U.S. Department of Energy.

Hydrologic Effects of Potential Changes in Climate, Water Use, and Land Cover in the Upper Scioto River Basin, Ohio

By Andrew Ebner, G.F. Koltun, and Chad J. Ostheimer

Abstract

This report presents the results of a study to provide information on the hydrologic effects of potential 21st-century changes in climate, water use, and land cover in the Upper Scioto River Basin, Ohio (from Circleville, Ohio, to the headwaters). A precipitation-runoff model, calibrated on the basis of historical climate and streamflow data, was used to simulate the effects of climate change on streamflows and reservoir water levels at several locations in the basin. Two levels of simulations were done. The first level of simulation (level 1) accounted only for anticipated 21st-century changes in climate and operations of three City of Columbus upground reservoirs located in northwest Delaware County, Ohio. The second level of simulation (level 2) accounted for development-driven changes in land cover and water use in addition to changes in climate and reservoir operations.

A statistical change-factor approach was used to construct future climate time series that were used in the precipitation-runoff model to compute time series of future streamflows and reservoir water levels. Monthly change factors were computed by determining differences or fractional changes between baseline historical climate time series and future climate time series consisting of outputs from selected global climate models that were included in the World Climate Research Programme's Coupled Model Intercomparison Project phase 3 (CMIP3). Eight sets of change factors were determined on the basis of outputs from four global climate models, each of which was run under two greenhouse-gas scenarios (the "A1b" and "A2" scenarios from the Intergovernmental Panel on Climate Change's 4th assessment). The 4 global climate models whose data were used in this study were selected to represent a wide range of potential climate outcomes as compared to the entire range of potential climate outcomes associated with the 16 global climate models represented in the CMIP3 multi-model dataset.

Future land-cover and water-use data were estimated for use in the level-2 precipitation-runoff simulations to account for development-driven changes in land cover and water use. Future land-cover characteristics were estimated for selected future years based on population projections and zoning plans for communities in the basin. Future water-use data for major water suppliers and wastewater-treatment facilities were estimated from current per capita water use, population projections for 2035, and population projections for 2090 assuming full build-out. A statistical change-factor-based approach was used to estimate future water-use characteristics by major water suppliers and wastewater-treatment facilities on the basis of reference-period historical water uses. Annual change factors that were determined for future years other than 2035 and 2090 (when the change factors could be explicitly computed) were estimated by interpolating or extrapolating linearly in time. Water uses by entities other than major water suppliers and wastewater-treatment facilities were assumed to remain unchanged because of uncertainty about if and (or) how they might change.

Results from the level-1 simulations were analyzed primarily to facilitate evaluation of climate-driven temporal changes in annual, seasonal, and monthly streamflow and water-level characteristics, as well as in maximum and minimum 7-, 30-, and 180-day average streamflow and reservoir water levels. Results from the level-2 simulations were analyzed to help evaluate and contrast (relative to level-1 results) the effects of the added development-related factors on maximums and minimum 7-, 30-, and 180-day average streamflows and reservoir water levels and duration characteristics of 7- and 30-day average streamflows and reservoir water levels. Results for 12 stream locations and 5 reservoirs in the Upper Scioto River Basin are presented primarily as a series of plots.

Although it is beyond the scope of this study to address results in detail for each model-output location, selected results are discussed to illustrate potential uses and interpretations of the graph products provided in this report. In addition, general trends and patterns in streamflow and water-level characteristics are identified where possible.

Introduction

In their fifth assessment report, the Intergovernmental Panel on Climate Change[1] (IPCC) stated that climate change is occurring in response to human activities (such as burning of fossil fuels and deforestation) and that climate change poses risks to both human and natural systems (IPCC, 2014). According to the IPCC (2014), effects of climate change that already have been observed include worldwide shrinkage of glaciers due to melting, warming and thawing of permafrost in regions of high altitude and high latitude, and alteration of hydrologic systems that affect runoff and water resources.

On the basis of the findings of the IPCC and other climate scientists, water managers and planners in central Ohio expressed concern about the potential effects of climate change on water resources. To help address those concerns, the U.S. Geological Survey (USGS)—in cooperation with the Mid-Ohio Regional Planning Commission; the Ohio Water Development Authority; the City of Columbus, Ohio; and Del-Co Water Company—undertook a study to investigate the potential effects of projected 21st-century changes in climate on streamflow and reservoir water-level characteristics in the Upper Scioto River Basin. The study used a precipitation-runoff model to estimate the site-specific hydrologic effects of 21st-century changes in climate as informed by selected Global Climate Models (GCMs). In addition to climate-driven changes, the added hydrologic effects of anticipated 21st-century changes in land cover and water use also were evaluated.

Description of Study Area

The Upper Scioto River Basin, located in west-central Ohio, covers an area of 3,219 square miles (mi^2) and represents nearly half the drainage of the 6,517-mi^2 Scioto River Basin (fig. 1). The basin drains a primarily rural, agricultural headwater area in the north with small pockets of urbanization from cities such as Bucyrus, Galion, Kenton, Marion, and Marysville. The basin is more heavily developed near the city of Delaware and the greater Columbus metropolitan area, and it is more rural south of Columbus to the terminus of the study area at Circleville, Ohio.

Based on the 2006 National Land Cover Database (Fry and others, 2011), the primary land cover in the basin is agriculture (66.3 percent) with some forest (11.6 percent). Development (20.2 percent) has occurred in urbanized pockets, with the vast majority in the greater Columbus metropolitan area. Only a small percentage (0.7 percent) is characterized as grasslands, wetlands, or open water. Population within the Upper Scioto River Basin, as based on the 2010 census (U.S. Census Bureau, 2014), is estimated at about 1.6 million people.

The Upper Scioto River Basin lies just west of the Allegheny Escarpment in the Till Plains physiographic region. The terrain varies from relatively flat in the north and northwest to rolling hills in the south and southeast (Ohio Division of Geological Survey, 1998). The rock strata underlying the Upper Scioto River Basin range in age from Silurian to Devonian (split north to south approximately along the western Franklin County boundary) with a sliver of Mississippian-aged rock along the eastern basin edge (split north to south east of the approximate western Fairfield County boundary) (Ohio Division of Geological Survey, 2006). The majority of soils within the basin are of glacial origin with soils in the Miamian and Blount catenas occurring in the glacial limestone area and the Bennington catena of soils occurring in the glacial sandstone and shale area (Schiefer, 2002).

The climate of central Ohio is continental, with an average annual temperature and precipitation of approximately 51 degrees Fahrenheit (°F) (10.6 degrees Celsius [°C]) and 39 inches, respectively (National Oceanic and Atmospheric Administration, 2014). Winter temperatures average about 30 °F (−1.1 °C) and summer temperatures average about 72 °F (22.2 °C). Basinwide average annual snowfall is approximately 22 inches.

Larger tributaries to the Upper Scioto River include the Little Scioto River, Mill Creek, the Olentangy River, Big Walnut Creek, Walnut Creek, and Big Darby Creek (fig. 1). Streamflow currently is regulated in the basin by five inline reservoirs: O'Shaughnessy Reservoir (Scioto River), Griggs Reservoir (Scioto River), Delaware Lake (Olentangy River), Hoover Reservoir (Big Walnut Creek), and Alum Creek Lake (Alum Creek) (fig. 1). In addition, a new upground reservoir[2] (John R. Doutt Reservoir), located near the Scioto River in Delaware County and small portion of Union County, Ohio, was completed in fall 2013. In order to help meet water-supply demands, the 9-billion-gallon John R. Doutt Reservoir can be filled from the Scioto River during periods with adequate streamflow and will release water back into the Scioto River during low-flow periods. Two more upground reservoirs (designated R-1 and R-3) are planned to help address water-supply needs. Combined, the R-1 and R-3 reservoirs are expected to have the potential to store about 8.7 billion gallons of water. Although no firm timeline has been established for the construction and filling of the R-1 and R-3 reservoirs, for this study, they are assumed to begin operation in 2040.

[1] The Intergovernmental Panel on Climate Change is a multinational scientific intergovernmental body that was established by the United Nations Environment Programme and the World Meteorological Organization to provide the world with information on the current state of knowledge about climate change and its potential environmental and socioeconomic impacts.

[2] Upground reservoirs are reservoirs that are formed by artificial barriers on two or more sides and which impound water pumped or otherwise imported from an exterior source.

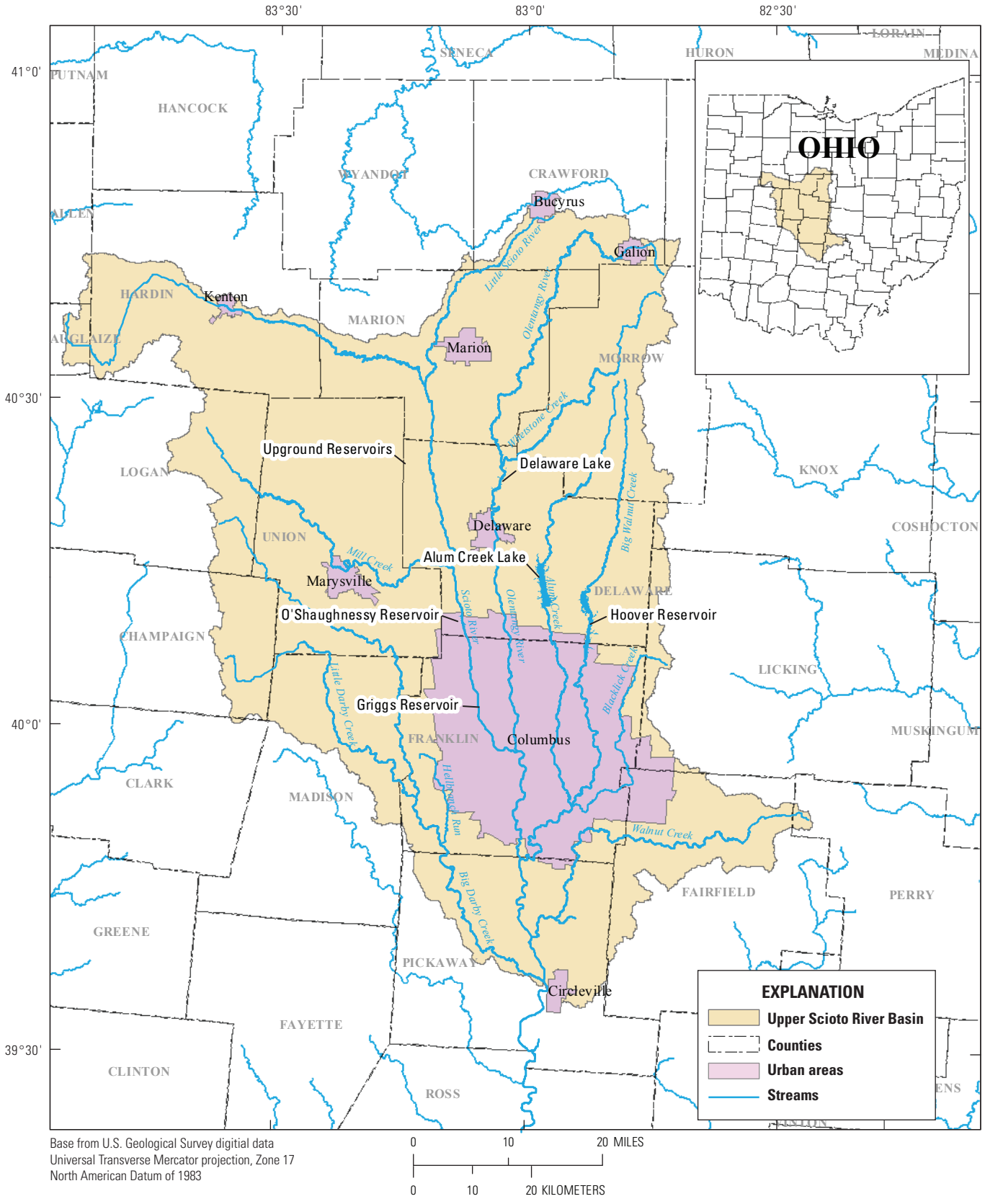

Figure 1. Upper Scioto River Basin and locations of major urban areas, primary streams, and inline reservoirs and lakes.

Purpose and Scope

The purpose of this report is to describe analytical methods and results of a study to provide information on the hydrologic effects of potential 21st-century changes in climate, water use, and land cover in the Upper Scioto River Basin, Ohio. The Hydrological Simulation Program—FORTRAN (HSPF) precipitation-runoff model (Bicknell and others, 2005), calibrated on the basis of historical climate and streamflow data, was used to simulate the effects of climate change (as indicated by selected global-climate-change models) on streamflows and reservoir water levels at several locations in the basin. Two levels of simulations were done. Level-1 simulations accounted only for anticipated changes in climate and operations of three City of Columbus upground reservoirs (the John R. Doutt Reservoir and two proposed reservoirs referred to as R-1 and R-3) in northwest Delaware County, Ohio. Results from the level-1 simulations were analyzed primarily to evaluate climate-driven temporal changes in annual, seasonal, and monthly streamflow and water-level characteristics as well as in maximum and minimum N-day (where N equals 7, 30, or 180) average streamflow and reservoir water levels. Level-2 incorporated development-driven changes in land cover and water use in addition to the level-1 changes in climate and reservoir operations. Results from the level-2 simulations were analyzed to evaluate and contrast (relative to level-1 results) the effects of these added development-related factors on N-day average streamflows and reservoir water levels.

Precipitation-Runoff Model of the Upper Scioto River Basin

HSPF (Bicknell and others, 2005) was used to simulate daily mean streamflows and reservoir water levels for selected locations in the Upper Scioto River Basin. HSPF uses meteorological data and model parameters representing basin geometry, land cover, soils, and hydrogeological characteristics to simulate the hydrologic responses that occur within the basin. To develop the model, the basin was subdivided into hydrologically similar areas referred to as hydrologic response units (HRUs) that drain to a network of river reach and reservoir (RCHRES) segments. HRUs typically are homogeneous with respect to land cover, soils, subsurface geology, and other characteristics that are expected to be fairly uniform with respect to their effect on potential evapotranspiration and hydrologic response to precipitation and snowmelt.

HSPF simulates most aspects of the hydrologic cycle, including interception, interflow, ground-water recharge, base flow, snowpack depth and water content, snowmelt, soil moisture, evapotranspiration, surface runoff, and channel and reservoir routing. HSPF can also account for water uses within the basin and can simulate river-basin management and reservoir operations based on operation rule sets and environmental conditions. The ability to simulate complex river-basin management and reservoir operations was particularly important in this project because of the need to account for the operation of eight reservoirs.

The HSPF model was developed by (1) creating a conceptual model to represent the hydrology of the basin, (2) discretizing the basin into HRUs, (3) compiling and processing input data and selecting initial model parameters, (4) calibrating the model (adjusting model parameters) on the basis of historical observed climate data, water uses, and hydrologic responses, and (5) evaluating the performance of the calibrated model against historical observations of streamflow not used for calibration purposes. The development of the HSPF model is described in more detail in appendix A.

Climate Data Used in the Model

The World Climate Research Programme's (WCRP's) Coupled Model Intercomparison Project phase 3 (CMIP3) multimodel dataset (Meehl and others, 2007) was the source of GCM data used for the analyses described below. Monthly bias-corrected, spatially downscaled (BCSD) datasets were downloaded from the GCM-archive Web site (http://gdo-dcp.ucllnl.org) that was developed by archive collaborators that included the Bureau of Reclamation, Climate Analytics Group, Climate Central, Lawrence Livermore National Laboratory, Santa Clara University, Scripps Institution of Oceanography, U.S. Army Corps of Engineers, and U.S. Geological Survey. A brief discussion of how the data on the GCM-archive Web site had been bias corrected and spatially downscaled is given below.

Comparisons of GCM simulation results for historical periods to observed climate data often showed biases (Bureau of Reclamation, 2013). Consequently, the raw GCM outputs were corrected to remove wet, dry, cool, and (or) warm biases that varied by location, season, and climate variable. A quantile-mapping technique operating on a monthly and location-specific basis that related modeled 20th-century cumulative distribution functions (CDFs) of precipitation and temperature to CDFs of observed 20th-century values was applied to bias-correct the 21st-century GCM data. This methodology effectively assumes that the GCM biases will have the same structure in the 20th- and 21st-century simulations. See Bureau of Reclamation (2013) for more information on the bias-correction methodology.

The bias-corrected GCM data originally were at a relatively coarse 2-degree resolution. In order to provide more spatially resolved data, the dataset was spatially downscaled to a 1/8-degree resolution. Observed 20th-century climate data were compared to GCM-simulated 20th-century climate data to compute change factors that reflect departures of observed spatial climatology from that of the climatology associated with the 2-degree coarse-resolution grid cells. The computed change factors were interpolated spatially by using a modified

Table 1. Greenhouse-gas emission scenarios for the Coupled Model Intercomparison Project phase 3 (CMIP3) multimodel datasets (IPCC, 2000).

Special Report on Emissions Scenarios designation	Description
A2	The A2 scenario represents a divided world that is characterized by— • A world of independently operating, self-reliant nations. • Continuously increasing population. • Regionally oriented economic development.
A1b	The A1b scenario represents a more integrated world that is characterized by— • Rapid economic growth. • A global population that reaches almost 9 billion in 2050 and then gradually declines. • The quick spread of new and efficient technologies. • A convergent world—income and way of life converge between regions. Extensive social and cultural interactions worldwide. • A balanced emphasis on all energy sources.
B1	The B1 scenarios represent a world that is more integrated and ecologically friendly characterized by— • Rapid economic growth as in A1b, but with rapid changes towards a service and information economy. • Population rising to almost 9 billion in 2050 and then declining as in A1b. • Reductions in material intensity and the introduction of clean and resource efficient technologies. • An emphasis on global solutions to economic, social and environmental stability.

inverse-distance-squared interpolation scheme, and then the interpolated change factors were used to compute the climatology at a 1/8-degree resolution. See Bureau of Reclamation (2013) for more information on the spatial downscaling methodology.

The BCSD CMIP3 datasets available on the GCM-archive Web site consisted of a 112-member ensemble of monthly temperature and precipitation projections for the period 1950–2099, representing 16 climate models and 3 of the Special Report on Emissions Scenarios (SRES) greenhouse-gas (GHG) scenarios featured in the IPCC report on emission scenarios (IPCC, 2000). The three GHG-emission scenarios (hereafter referred to as "emission scenarios") used to compute the BCSD CMIP3 datasets were the SRES A1b, A2, and B1 scenarios (table 1). The time series of worldwide anthropogenic carbon dioxide (CO_2) emissions and populations on which these emission scenarios were based are illustrated in figures 2 and 3.Although the CMIP3 datasets contain results for three emission scenarios, the decision was made to use only data from the A2 and A1b scenarios for analysis. That decision was made by the USGS and its study partners based on the need to make the best use of project resources and on current worldwide political trends that suggest that the world view expressed by the B1 scenario may be overly optimistic and, consequently, less likely to occur.

The ensemble of GCM outputs on the GCM-archive Web site exhibit a wide range of potential climate outcomes; however, there is no scientific consensus as to which of the GCMs is likely to be most accurate (Hay and others, 2014). All of the GCMs forecasted increasing temperatures (although to varying degrees) for central Ohio for the A2 and A1b scenarios; however, there was no such consistent agreement on the trend in precipitation. Given the relatively wide range of results from the GCMs and uncertainty about the models, the USGS and partner agencies felt it prudent to consider the uncertainty represented by a subset of GCMs representing a range of outcomes.

A total of eight GCM/emission-scenario combinations consisting of four unique GCMs (table 2), each using the A2 and A1b emission scenario climate forcings, were selected for the analyses. This was done to limit the number of rainfall-runoff simulations to a set that was computationally manageable while still fulfilling the project goal of examining the effects of a range of potential climate outcomes. Two primary criteria were used to select the GCMs: (1) the selected GCMs spanned a wide range of projected outcomes with respect to temperature and precipitation and (2) the selected GCMs had temperature and precipitation variability characteristics that spanned a wide range of the variability characteristics present in the full ensemble of GCM outputs. Scatterplots (not shown) of means and standard deviations of all GCM-simulated air temperature versus precipitation along with maps of departures of end-of-21st-century temperatures and precipitation (fig. 4) were used to aid in meeting the selection criteria. Table 2 provides information on where the selected GCMs fall relative to each other in the spectrum of late 21st century (2080s) precipitation and temperatures (with a rank of 1 being the wettest or warmest of the group).

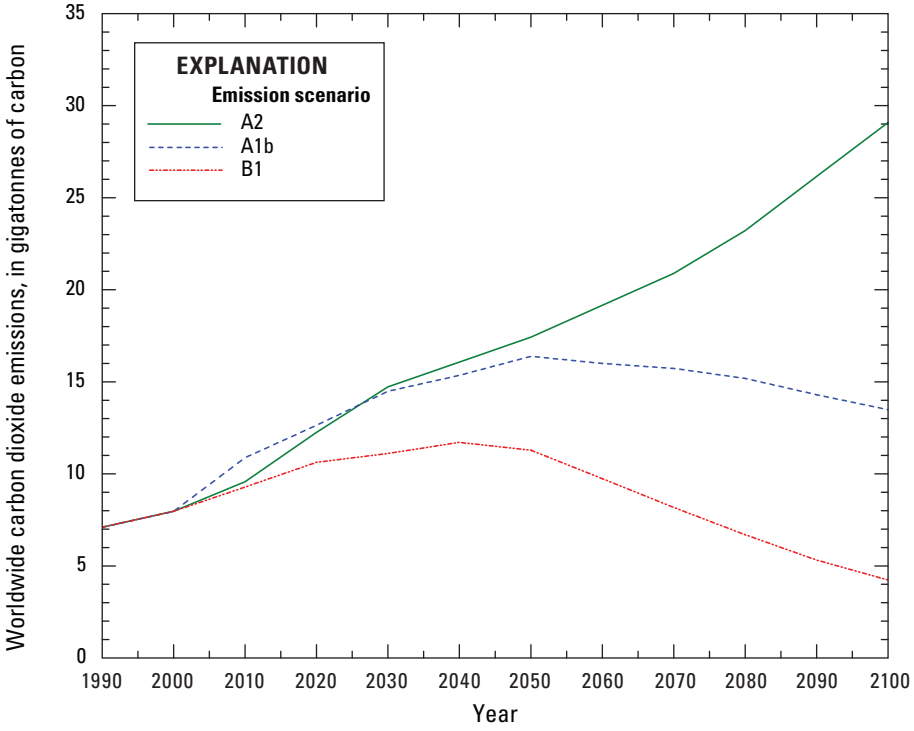

Figure 2. Projected anthropogenic carbon emissions for the A2, A1b, and B1 emission scenarios described in the Special Report on Emissions Scenarios (IPCC, 2000).

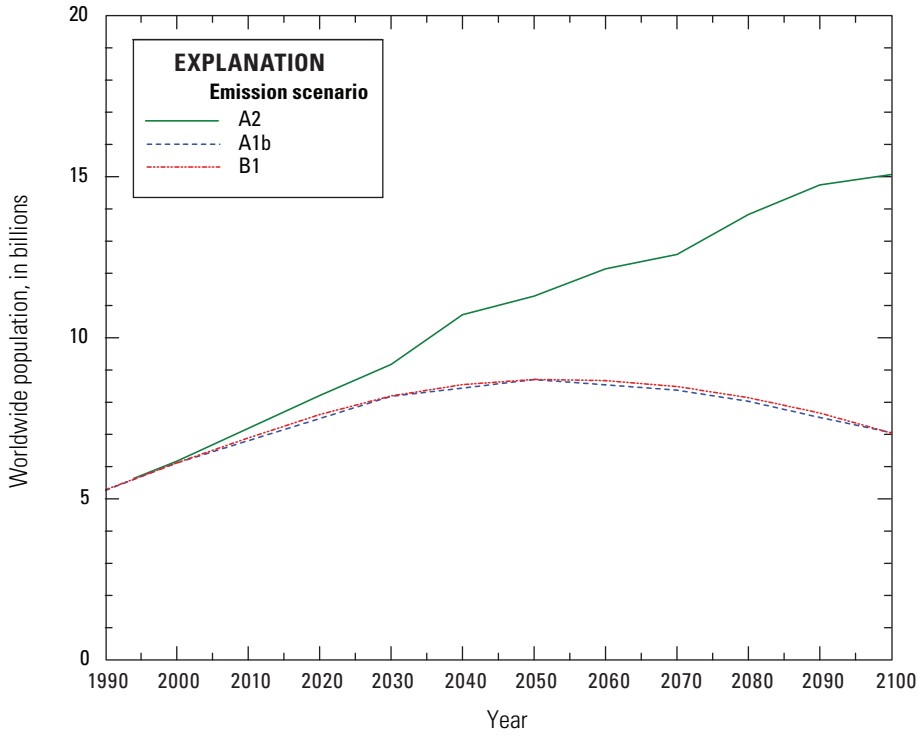

Figure 3. Projected worldwide populations for the A2, A1b, and B1 emission scenarios described in the Special Report on Emissions Scenarios (IPCC, 2000).

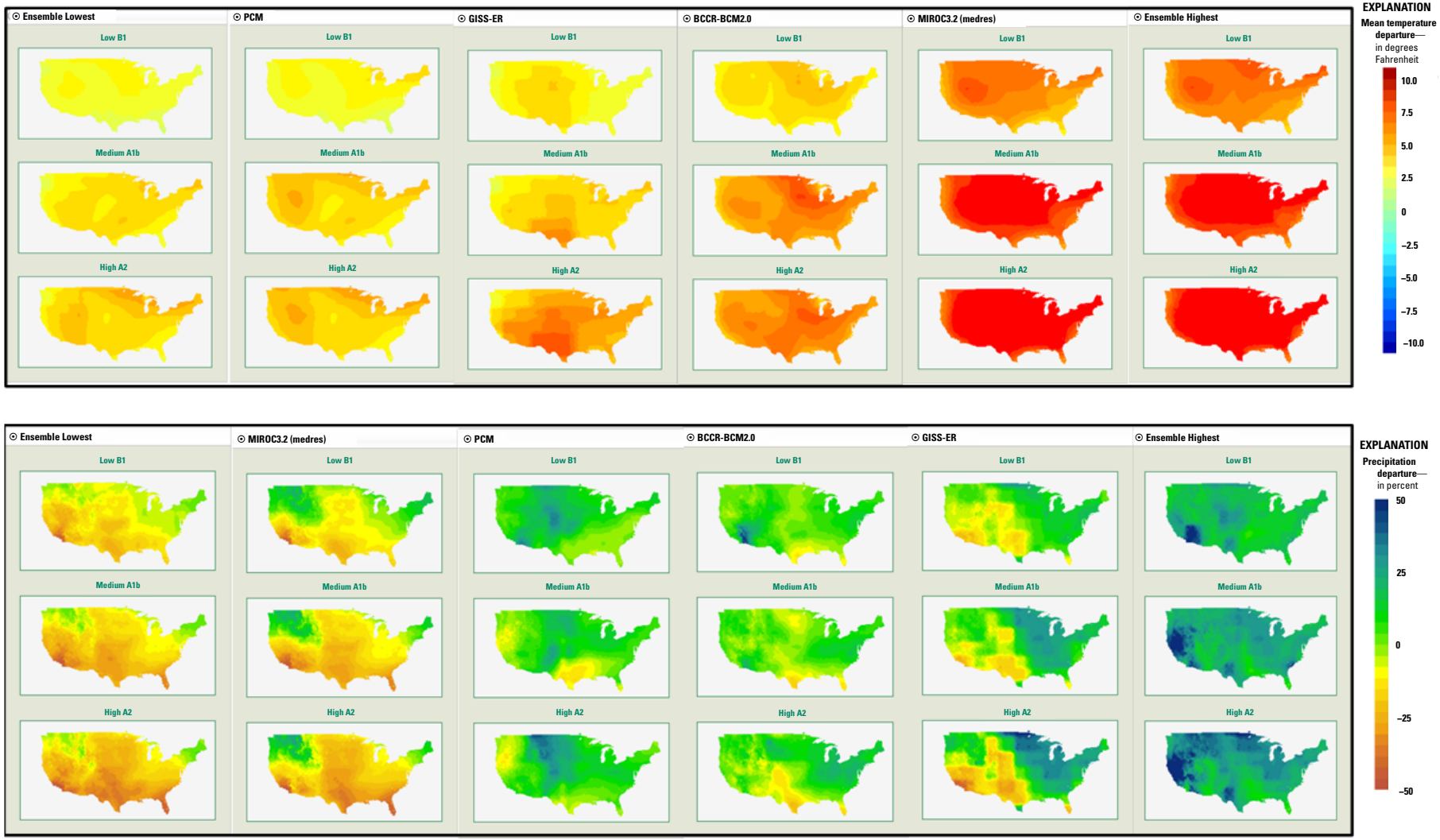

Figure 4. End-of-21st-century (2080s) departures (as compared to a 1961–1990 climate baseline period) in mean air temperature (top set) and precipitation (bottom set) for global climate models used in this study as compared to the lowest and highest departures for the entire ensemble of models in Coupled Model Intercomparison Project phase 3 dataset (top, middle, and bottom row of each set corresponds to the B1, A1b, and A2 emission scenarios, respectively). (Images mosaicked from ClimateWizard, 2012.)

Table 2. Global climate model results used in this study.

[CMIP3, Coupled Model Intercomparison Project phase 3; USA, United States of America; wet rank is rank order amongst selected models based on projected 2080s precipitation departure relative to the 1961–1990 period, where 1 means wettest and 4 means driest; warm rank is rank order amongst selected models based on projected 2080s air temperature departure relative to the 1961–1990 period, where 1 means warmest and 4 means coolest]

Originating group(s)	Country	CMIP3 identifier	Wet rank	Warm rank
Bjerknes Centre for Climate Research	Norway	BCCR-BCM2	3	2
NASA / Goddard Institute for Space Studies	USA	GISS-ER	4	3
Center for Climate System Research (The University of Tokyo) National Institute for Environmental Studies and Frontier Research Center for Global Change	Japan	MIROC3.2	1	1
National Center for Atmospheric Research	USA	NCAR-PCM	2	4

Tests were done to determine a simulation time step at which the HSPF model could reasonably reproduce the observed hydrology for the calibration/validation period extending from 1991 to 2010 (hereafter referred to as the "reference period"). Both daily and hourly time steps were tested, and it was determined that good model calibration could be obtained by using an hourly time step but not a daily time step. Factors such as the relatively small drainage areas of some of the calibration subbasins along with the ability to better simulate reservoir operations in the model at hourly versus daily time steps influenced this result.

In order to run the HSPF model at an hourly time step, hourly climate data are necessary; however, the CMIP3 datasets are available only at monthly and daily time steps. Neither the monthly nor daily CMIP3 datasets could be used directly in the HSPF model (owing to incompatible time steps) and temporal disaggregation of the daily GCM data to an hourly time step was ruled out (primarily because of concerns about the representativeness of temporally disaggregated precipitation data). Consequently, a simple statistical change-factor (or delta) approach was adopted to provide climate data for the HSPF model. The statistical change-factor approach has been used successfully in several previous studies, recent examples of which include Hay and McCabe (2010) and Markstrom and others (2012). Although there is active debate about the merits of dynamical versus statistical downscaling methods, Fowler and others (2007) reviewed both methods for applicability to hydrological modeling and concluded that the more complex dynamical methods (such as inset regional climate models or limited-area models) provided little advantage over simple statistical downscaling methods, such as the change-factor method. It is worth noting, however, that the change-factor method scales the climatic variables but does not alter their temporal sequence. So, for example, if a GCM indicates that the durations of consecutive dry or wet days will change appreciably in the future, those pattern changes will not be reflected in the change-factor adjusted climate (although their effects on monthly total precipitation, if any, will be represented).

In the statistical change-factor approach, differences or fractional changes between historical baseline and future GCM simulations (change factors) are computed and applied to historical climate observations simply by adding to or multiplying the observations by the change factor computed for the future date(s). Location-specific change factors were computed for future months for each GCM/emission combination by (1) computing mean monthly temperatures and precipitation from GCM-simulated results for a historical baseline period (1980–1999), (2) computing time-centered mean monthly temperature and precipitation values for all GCM-simulated future months by applying a time-centered 11-year-moving-average window operating separately on each calendar month (for example, the average January 2020 temperature would be determined by averaging January temperatures for the 11 years ranging from 2015 to 2025 and the average January 2021 temperature would be determined by averaging January temperatures for the 11 years ranging from 2016 to 2026, and so forth), and then (3) from those time-centered averages, computing change factors by subtracting the baseline GCM mean monthly values (in the case of temperature) or dividing by mean monthly values (in the case of precipitation). Change factors were computed for locations corresponding to each climate station whose data were used as input to the HSPF model. For example, figures 5 and 6 show time series of the precipitation and air-temperature change factors that were computed for the location corresponding to the Columbus, Ohio, climate station (Columbus WSO AP). It is apparent from figures 5 and 6 that there is no consistent temporal trend in monthly precipitation amongst all of the GCMs; however, all of the GCMs indicate increases in monthly mean air temperatures by the end of the 21st century (although to varying degrees).

Climate change factors were applied to the observed climate time series (at climate stations listed in table 3) for the period 1989–2010 to create future climate time series. Each observation in the observed climate time series was time shifted by adding a year offset value. For example, if the observed climate time series was used to create a future climate time series beginning in 2020, then 31 years (1989 + 31 = 2020) was

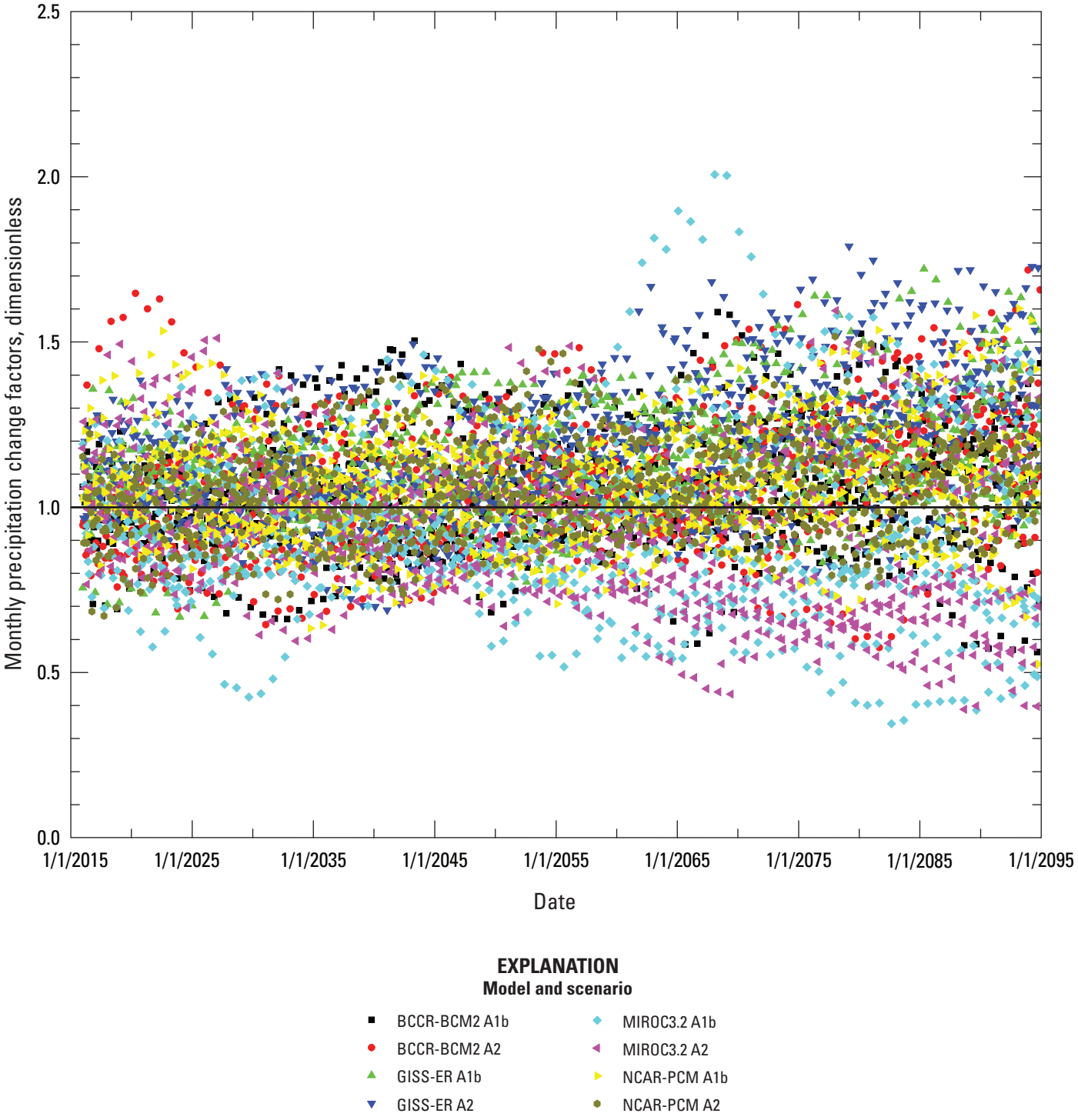

Figure 5. Monthly precipitation change factors relative to the climate baseline period 1980–1999 computed from global climate model outputs for the Columbus, Ohio, area. (Abbreviations for models and scenarios are defined in tables 2 and 1, respectively.)

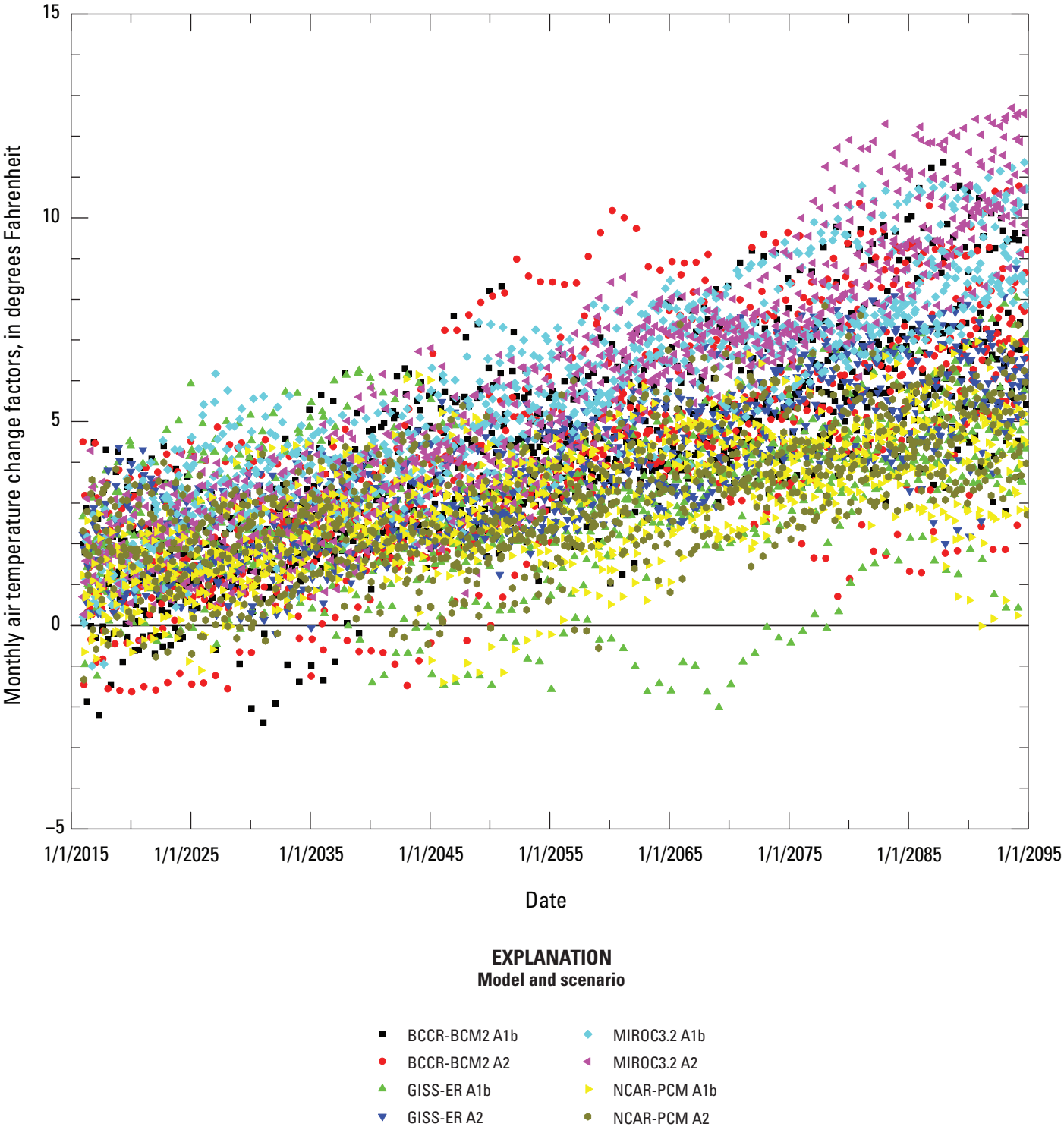

Figure 6. Monthly air-temperature change factors relative to the climate baseline period 1980–1999 computed from global climate model outputs for the Columbus, Ohio, area. (Abbreviations for models and scenarios are defined in tables 2 and 1, respectively.)

Table 3. Climate stations and types of data used in this study.

[NOAA, National Oceanic and Atmospheric Administration; P, hourly precipitation data; T, hourly air temperature data; data retrieved for all stations were for the period 1989–2010]

NOAA station number	Station name	Decimal latitude	Decimal longitude	Type(s) of data used
OH331404	Centerburg 2 SE	40.30	−82.65	P
OH331592	Circleville	39.62	−82.95	P
OH331786	Columbus WSO AP	39.98	−82.87	P,T
OH332090	Deer Creek Lake	39.63	−82.22	P
OH332124	Delaware Lake	40.37	−84.07	P
OH333021	Galion Wtr Wks	40.63	−82.82	P
OH334189	Kenton	40.65	−83.65	P
OH334403	Lancaster	39.72	−82.60	P
OH334942	Marion 2 N	40.62	−83.13	P,T
OH334979	Marysville	40.23	−83.37	P

added to each date in the observed climate time series. Once the observed climate time series data were time shifted, they were adjusted by the change factors computed for the time of each time-shifted observation. Because change factors were computed as monthly values, all hourly values at a given location for a given month in the future were adjusted by a common monthly change factor. Of course, the change factors for a given month in the future varied depending on (a) which climate variable was being processed, (b) the location, and (c) the GCM/emission combination being processed.

The observed climate time series was used to generate an ensemble of seventy-seven 22-year-long future climate time series with start dates beginning in 2016 and sequentially incrementing by 1 year through 2092. As a result, for example, the observed climate time-series data for January 1, 1989, was used to generate future climate time-series data for January 1 of years 2016 through 2092. Depending on the year offset, a given day in the future could have up to 20 realizations[3] of hourly climate data—one based on that calendar day's climate data occurring in each of the years in the observed climate time series (minus the first 2 years of data that were omitted to initialize the model). Using multiple realizations of climate helped to account for natural year-to-year variability in climatic conditions during subsequent analyses.

Water-Use Data Used in the Model

Monthly surface-water withdrawal information for the period 1990–2010 was obtained from the Ohio Department of Natural Resources (ODNR) Water Withdrawal Facilities Registration Program (WWFRP) for public water supplies; agricultural, landscaping, commercial, and industrial users; and golf courses. In all, 84 unique withdrawals were simulated in the HSPF model. If a subbasin contained more than one golf course, agriculture, or landscaping withdrawal, those withdrawals were combined into a single withdrawal time series in the model. Unless otherwise indicated, the effects of groundwater withdrawals on groundwater discharge to streams and (or) induced infiltration from streams to groundwater sources were not directly accounted for in the model.

Monthly withdrawals were disaggregated into daily values by assuming a constant withdrawal rate. Daily values were then disaggregated into hourly values by assuming a constant rate of withdrawal for all withdrawals other than golf courses and agricultural withdrawals, which were disaggregated to have withdrawals occur only between the hours of 7:00 p.m. and 6:00 a.m., when irrigation would be most likely to occur. More detail about withdrawals can be found in appendix A.

Data on return flows were obtained from two sources, the ODNR WWFRP and the National Pollutant Discharge Elimination System (NPDES). Monthly return-flow time series obtained from the ODNR WWFRP were disaggregated into hourly values by assuming a constant rate of return. Daily wastewater-treatment-plant discharge time series obtained from the NPDES also were evenly disaggregated into hourly values (in spite of the fact that wastewater-treatment-plant discharges typically exhibit diurnal variation). Only data for wastewater-treatment plants designated as major facilities (that is, those with design flows of 1 million gallons per day or greater, or facilities with EPA/State approved industrial pretreatment programs) were considered for this study. In all, return-flow information was obtained for 38 unique entities. More detail about return flows can be found in appendix A.

Future changes in selected water uses were considered for some analyses. Specifically, an attempt was made to reflect anticipated future changes in withdrawals and return flows associated with development for major water suppliers and wastewater-treatment facilities. Although one might expect that there could also be changes in withdrawals for irrigation

[3]A "realization" is a model result determined by using a change-factor-adjusted climate time series computed from a specific year of historical climate record.

or certain industrial activities as a result of climate change, those water uses were held constant because of uncertainty about how those changes might occur.

The engineering firm of Brown and Caldwell, with input from the Mid-Ohio Regional Planning Commission (MORPC), provided estimates of current (1990–2010), 2035, and 2090 withdrawals and return flows for major facilities, including those serving the cities of Canal Winchester, Columbus, Delaware, Galion, Kenton, Marion, Marysville, and counties of Delaware, Fairfield, and Marion (tables 4 and 5). Water-use estimates for 2035 were developed by using population projections provided by the Mid-Ohio Regional Planning Commission and current per capita water usage for each of the major facilities. Water-use estimates for 2090 were based on the population that would exist in the region if each municipality were to fully develop as per its existing zoning (a situation referred to as "build-out") and with current per capita water usage. Changes in estimates of future water use relative to current water use were used to scale a total of 25 of the 1990–2010 observed water-use time series to account for anticipated future increases or decreases in withdrawals and return flows. The remaining 59 time series of water uses were not scaled; rather, the water-use rates computed for the 1990–2010 period were held constant for the future-climate scenarios.

Water-use change factors were computed for 2035 and 2090 by taking the ratio of the estimated water use in those years to the water use in 2010. For example, the 2035 withdrawal for the City of Delaware is estimated to increase by a factor of about 1.49 (5.35/3.60 = 1.49) relative to the 1990–2010 withdrawal. That factor, for example, would be multiplied by the observed 2010 time series of withdrawals for the City of Delaware to estimate a comparable time series of withdrawals for the year 2035. By definition, change factors associated with 2010 are all 1.0. Water-use values used to compute change factors for years other than 2010, 2035, and 2095, were computed by linear interpolation or extrapolation by assuming constant rates of change in water use between sets of years closest in time. When extrapolating water-use values for a given location for years earlier than 2010, 80 percent of the 2010 value was used as the minimum water-use value. The 80-percent reduction threshold was chosen to better replicate the historically observed water uses for the period 1990–2010 which otherwise would have been underestimated by the extrapolation process (due to a slower rate of change in water use during the historical period as compared to the rate of change anticipated in future years).

Similar to the climate time series, a change-factor approach was used with observed water-use time series to generate ensembles of future water-use time series with start years beginning in 2016 and sequentially incrementing by 1 year through 2092. Each observation in the observed water-use time series was time shifted by adding a year offset value. Once the observed water-use time series data were time shifted, water uses associated with the major water supplies and wastewater-treatment facilities were adjusted by applying change factors where the time associated with each observation in the time-shifted dataset was used to look up the appropriate water-use change factor.

Land-Cover Data Used in the Model

Land-cover data were used along with other data (such as soils and land-surface elevation data) in the HSPF model to help discretize the basin into hydrologic response units (HRUs). Land-cover data also were used within the HSPF model to define the spatial variation in model parameters that affect a variety of hydrologic processes such as infiltration, evapotranspiration, and runoff.

The 2006 National Land Cover Database (NLCD) (Fry and others, 2011) was used as the basis for determining land cover for the reference period. The 2006 NLCD contains 20 land-cover classifications, 15 of which are found in the Upper Scioto River Basin. These 15 land-cover classifications were reclassified into the following 9 classifications: (1) open water, (2) developed, open space; (3) developed, low intensity; (4) developed, medium intensity; (5) developed, high intensity; (6) forest; (7) grassland herbaceous; (8) agriculture; and (9) wetlands.

Geospatial data describing how land cover is anticipated to change with future development was provided by MORPC (Nancy Reger, Mid-Ohio Regional Planning Commission, unpub. data, 2013). MORPC provided Geographic Information System (GIS) datasets of land cover in the Upper Scioto River Basin reflecting anticipated development conditions in 2035 and full build-out in 2090 as per current zoning. MORPC created those datasets by obtaining zoning plans from the local communities and translating those plans into spatial land-cover datasets employing the land-cover classifications used in the HSPF model. With the exception of the Little Scioto River Basin, most of the development is expected to occur in the lower two-thirds of the Upper Scioto River Basin.

The land-cover datasets provided by MORPC primarily showed agricultural land cover being converted to land covers associated with development. For example, the percentage of land cover in the Upper Scioto River Basin classified as agriculture decreased from about 66.3 percent in 2010 to 63.6 percent in 2035 and 58.0 percent in 2090 while at the same time the total of land covers classified as developed increased from about 20.2 percent in 2010 to 22.8 percent in 2035 and 28.5 percent in 2090. The Mill Creek Basin, which contains the city of Marysville, had the largest projected percentage increase in developed land cover, with developed area in the basin increasing from about 14 percent in 2020 to about 22 percent in 2035 and 47 percent in 2090.

The land-cover datasets provided by MORPC were used in a GIS to recompute the areas and average elevations associated with the various land-cover classifications within each HRU in 2035 and 2090. For computational purposes, the 2035 land-cover data were assumed to be representative of the period 2025–2045. Land cover for intermediate years of

Table 4. Withdrawals by municipal water suppliers in the upper Scioto River Basin.

[Mgal/d, million gallons per day; data source: Kristin Knight, Brown and Caldwell, written commun., 2014]

Utility	Percentage of water supplied from groundwater	Average daily surface-water demand, 1990–2010 (Mgal/d)	Projected average daily surface-water demand, 2035 (Mgal/d)	Projected average daily surface-water demand at build-out, 2090 (Mgal/d)
City of Columbus – Service Area	17	142.39	148.45	292.32
City of Westerville	5	3.80	4.49	5.00
City of Delaware	15	3.60	5.35	6.30
Del-Co - Ralph E. Scott	0	3.08	6.83	12.89
Del-Co - Olentangy	0	7.72	17.24	23.32
City of Marysville	46	1.93	3.65	8.97
Aqua Ohio - Marion	35	6.23	4.64	8.14
City of Galion	0	1.06	1.11	1.65

Table 5. Municipal wastewater-treatment-plant return flows in the upper Scioto River Basin.

[Mgal/d, million gallons per day; RSD, regional sewer district; WRC, water reclamation center; WRF, water reclamation facility; WWTP, wastewater-treatment plant; return flows reported as sum of City of Columbus Southerly and Jackson Pike flows for 2035 and 2090; data source: Kristin Knight, Brown and Caldwell, written commun., 2014]

Utility	Average daily flow rate, 2010 (Mgal/d)	Projected average daily flow rate, 2035 (Mgal/d)	Projected average daily flow fate, 2090 (Mgal/d)
City of Columbus - Southerly	84.31	225.5	376.2
City of Columbus - Jackson Pike	69.00		
City of Delaware - Upper Olentangy WRC	4.50	7.87	9.26
City of Marysville	4.00	14.01	34.45
City of Marion	8.50	9.74	17.08
City of Galion	2.70	2.84	4.22
City of Kenton	1.20	1.26	3.53
City of Canal Winchester	2.48	4.08	9.35
City of Pickerington	3.20	4.96	9.00
Delaware County RSD - Alum Creek WRF	4.8	8.01	9.03
Delaware County RSD - Olentangy Environmental Control	3.00	6.49	7.97
Marion County Regional Sewer District No. 7	1.21	1.53	3.35
Fairfield County - Tussing Road WWTP	1.40	2.84	3.53

2055 (assumed representative of the period 2045–2065) and 2075 (assumed representative of the period 2065–2085) were interpolated on the basis of the assumption of a linear change in land cover and its associated elevations as a function of time between the 2035 and 2090 values. The GIS-computed and interpolated areas and average elevations of land-cover classifications were then used to revise the HSPF model and create three separate models to reflect each of the land-cover conditions for 11-year simulations of future time periods centered on the years of 2035, 2055, and 2075. Eleven-year-long periods were chosen with the intent that model results would approximately reflect the effects of the land-cover characteristics anticipated for the center year. Collectively, the years 2035, 2055, and 2075 will hereafter be referred to as "target years" because the anticipated land-cover characteristics for those years will be targeted to assess the hydrologic impacts of development-related changes in land cover. Each of the newly created models was run with the eight previously described GCM/emission-scenario combinations.

Description of HSPF Model Runs

The HSPF model was run to reflect two levels of complexity with respect to future conditions in the Upper Scioto River Basin. First, simulations were done to account only for changes in climate and anticipated operations of three City of Columbus upground reservoirs (John R. Doutt, R-1, and R-3 reservoirs) located in northwest Delaware County, Ohio. These simulations will be referred to as "level-1" simulations. Second, simulations were done to incorporate population and development-driven changes in land cover and water use in addition to the level-1changes in climate and reservoir operations. This second set of simulations will be referred to as "level-2" simulations.

For both the level-1 and level-2 simulations, the model was run 616 times: 77 times (once with each time series of time-shifted climate data beginning in years 2016 through 2092) for each of the 8 GCM/emission-scenario combinations. Each of those runs involved simulating hydrology with the HSPF model at an hourly time step for up to a 22-year period and outputting time series of daily mean values of streamflow or water level for 17 locations in the Upper Scioto River Basin (table 6 and fig. 7). For convenience, the output from HSPF simulations based on climate data for a given GCM and emission scenario will be referred to as a "GCM/emission-scenario output." Because initial hydrologic conditions typically are not known (particularly for simulations of future conditions), the first 2 years of each simulation were used to initialize the model and establish a realistic water balance within the basin. The 2 initialization years of results for each simulation were excluded from analyses, leaving 20 years of usable data.

Table 6. Precipitation-runoff model output locations.

[-, not applicable; sites are listed in alphabetical order by site ID]

Site ID	Description	Latitude	Longitude	Collocated streamgage[1]
AFRI	Alum Creek at Africa, OH	40°10'56"	82°57'41"	03228805
ALUM	Alum Creek Reservoir, OH	40°11'11"	82°57'59"	-
CBUS	Scioto River at Columbus, OH	39°54'34"	83°00'32"	03227500
CCOL	Big Walnut Creek at Central College, OH	40°06'12"	82°53'02"	03228500
CIRC	Scioto River at Circleville, OH	39°36'05"	82°57'18"	03230700
CLAR	Olentangy River at Claridon, OH	40°34'59"	82°59'22"	03223000
DELA	Olentangy River near Delaware, OH	40°21'18"	83°04'05"	03225500
DELL	Delaware Lake, OH	40°21'31"	83°04'09"	-
GRIG	Griggs Reservoir, OH	40°00'58"	83°05'38"	-
HOOV	Hoover Reservoir, OH	40°06'30"	82°52'53"	-
LSCI	Little Scioto River at mouth, OH	40°31'21"	83°12'20"	-
MILL	Mill Creek near Bellepoint, OH	40°14'55"	83°10'26"	03220000
OLEN	Olentangy River at mouth, OH	39°57'54"	83°01'01"	-
OLOC	Olentangy River near Olentangy Caverns, OH	40°11'55"	83°03'09"	-
OSHY	O'Shaughnessy Reservoir, OH	40°09'14"	83°07'32"	-
PROS	Scioto River near Prospect, OH	40°25'10"	83°11'50"	03219500
SROR	Scioto River at confluence with Olentangy River	39°57'54"	83°01'01"	-

[1] See appendix table A5 for more information on streamgages.

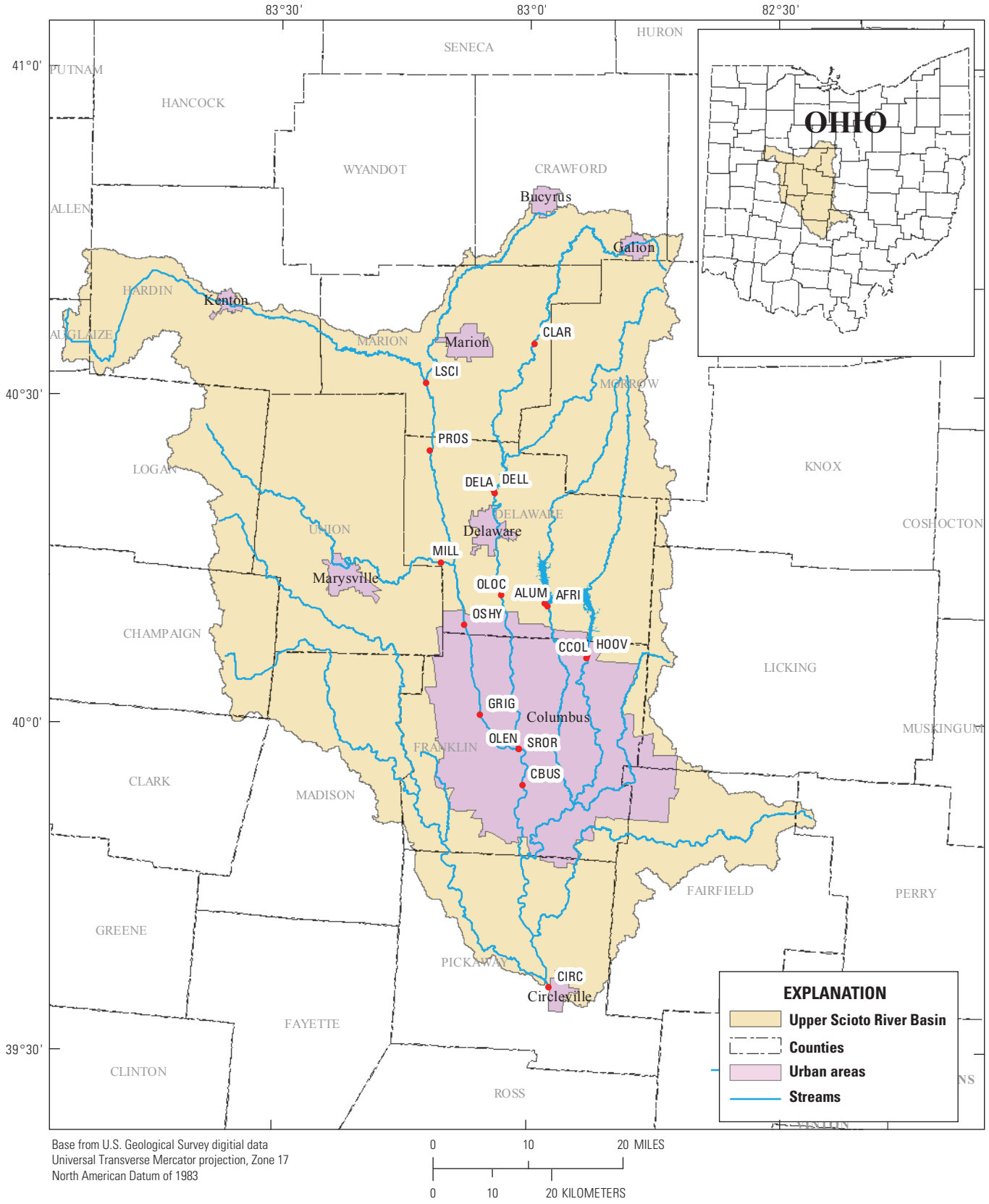

Figure 7. Upper Scioto River Basin and HSPF model-output locations.

Methods Used to Analyze Precipitation-Runoff Model Results

Time-series results from the HSPF level-1 simulations were analyzed primarily to evaluate climate-driven temporal changes in annual, seasonal, and monthly streamflow and reservoir water-level characteristics as well as in maximum and minimum 7-, 30-, and 180-day average streamflow and reservoir water levels. In addition to effects of climate change, level-1 simulations also include the effects of anticipated operations of the one existing and two proposed City of Columbus upground reservoirs. Time-series results from the HSPF level-2 simulations were analyzed to evaluate the effects of development-driven changes in land cover and water use in combination with the effects of changes in climate and upground-reservoir operations.

Statistical Analysis Overview

All statistical analyses were done by using Version 9.3 of the Statistical Analysis System (SAS Institute Inc.). Basic summary statistics (for example annual and monthly means) and duration characteristics were computed by using the UNIVARIATE procedure (SAS Institute Inc., 2014a). Duration quantiles were computed by using the type 4 quantile estimator option of the UNIVARIATE procedure (SAS Institute Inc., 2014a). The SAS type 4 quantile estimator is an L-moment-type estimator that provides weighted averages of adjacent order statistics (Vogel and Fennessy, 1994). Running N-day averages were computed with the EXPAND procedure (SAS Institute Inc., 2014b) by using the "trimleft" and "nomiss" options to ensure that all values were computed on the basis of the intended averaging period.

Analysis of Annual and Monthly Mean Streamflows and Reservoir Water Levels

Annual mean and monthly mean streamflows or water levels for the 17 model-output locations (fig. 7) were computed for each of the 616 level-1 simulations. For a given GCM/emission-scenario output, the number of annual mean or monthly mean streamflows or water levels computed for a future year and (or) month ranged from 1 to 20 realizations because of overlap of the time-shifted simulations. Grand means (determined by computing the mean of the ensemble of annual or monthly mean streamflows or water levels determined for a given year or month) were determined, and results for years or months based on less than 20 realizations were omitted. The retained grand means will hereafter be referred to as "ensemble means." An example of the data structure described above is shown in table 7 for annual mean streamflows computed from HSPF outputs for model output location, Alum Creek at Africa, Ohio, based on the BCCR-BCM2 GCM with the A1b emission scenario. Some rows and columns have been omitted to permit display on one page. Note that 2037 was the first year that ensemble means could be computed from the maximum complement of N=20 realizations.

For each model output location, eight time series of ensemble means (one for each of the eight GCM/emission-scenario outputs) were merged into one dataset and then time series of medians of the ensemble means were computed separately for the A1b and A2 emission-scenario outputs (for example, see table 8). Medians were used instead of means to represent central tendencies of the A1b and A2 emission scenarios because they are less influenced by outliers.

For each of the 17 model-output locations, plots were prepared showing time series of ensemble means of annual mean streamflows or water levels computed for the individual GCM/emission-scenario outputs and time series of the median of the ensemble means computed separately for the A1b and A2 GCM/emission-scenario outputs. An example plot of ensemble means of annual mean streamflows for model-output location AFRI (Alum Creek at Africa, Ohio) is shown in figure 8. Comparable plots for other model-output locations can be found in appendix B. A dashed horizontal line corresponding to the mean annual streamflow or water level determined from simulation results for the reference period was plotted on each graph to permit comparisons with future-period simulation results. To facilitate those comparisons, the reference-period line is shown as spanning the time period of the level-1 results (2037–2094) even though the statistics for the reference period are based on simulation results for the period 1991–2010 (the reference period).

Table 7. Example of data structure and statistics of annual mean streamflows computed from HSPF model output for Alum Creek at Africa, Ohio (AFRI), for simulations based on the BCCR-BCM2 GCM with the A1b emission scenario.

[…, intervening data not shown; max, maximum; min, minimum; N, number of observations]

Usable data begin year	Annual mean streamflow (in cubic feet per second) for indicated beginning year of simulation										Statistics of ensemble			
	2016	2017	2018	2019	2020	2021	…	2090	2091	2092	max	min	mean	N
2018	71.7						…				71.7	71.7	71.7	1
2019	11.6	72.9					…				72.9	11.6	42.3	2
2020	76.0	11.6	73.5				…				76.0	11.6	53.7	3
2021	55.9	86.0	11.6	71.9			…				86.0	11.6	56.4	4
2022	93.9	65.3	87.0	11.7	81.8		…				93.9	11.7	67.9	5
2023	193.8	84.1	63.6	98.9	11.6	80.6	…				193.8	11.6	88.8	6
…	…	…	…	…	…	…	…	…	…	…	…	…	…	…
2036	91.3	104.9	165.1	102.4	122.9	186.8	…				217.0	11.7	105.2	19
2037	108.4	102.5	111.2	182.6	115.2	136.6	…				230.3	11.7	114.1	20
2038		109.8	105.2	108.4	185.1	114.5	…				225.3	11.7	117.6	20
2039			104.9	95.1	103.2	170.2	…				218.8	11.7	110.5	20
2040				99.4	88.1	98.8	…				200.9	11.7	102.4	20
2041					96.7	66.6	…				193.6	11.7	94.8	20
2042						93.0	…				198.7	11.7	93.7	20
…	…	…	…	…	…	…	…	…	…	…	…	…	…	…
2092							…	83.0			166.9	11.6	78.5	20
2093							…	11.6	82.2		164.9	11.6	78.4	20
2094							…	61.8	11.6	87.5	163.2	11.6	77.4	20

Table 8. Example of data structure and statistics for the ensemble mean of annual mean streamflows computed from eight GCM/emission-scenario outputs for the Alum Creek at Africa, Ohio (AFRI) model output location.

[GCM, global climate model; …, intervening data not shown]

Year	Ensemble mean of annual mean streamflows (in cubic feet per second) for indicated GCM/emission-scenario outputs								Medians for indicated emission scenarios	
	BCCR-BCM2		GISS-ER		MIROC3.2		NCAR-PCM		A1b	A2
	A1b	A2	A1b	A2	A1b	A2	A1b	A2		
2037	114.1	92.4	108.2	114.3	63.6	66.2	96.2	102.6	102.2	97.5
2038	117.6	91.4	110.6	115.9	63.1	65.3	96.9	99.9	103.7	95.7
2039	110.5	92.8	120.9	115.2	62.7	69.2	99.5	105.3	105.0	99.1
2040	102.4	88.0	122.2	118.4	62.8	62.2	102.7	99.7	102.6	93.8
…	…	…	…	…	…	…	…	…	…	…
2092	78.5	121.4	158.0	181.8	39.9	31.8	109.0	121.5	93.8	121.4
2093	78.4	128.0	160.7	182.0	42.0	31.0	115.6	111.8	97.0	119.9
2094	77.4	127.4	166.6	188.6	41.7	33.6	120.0	113.4	98.7	120.4

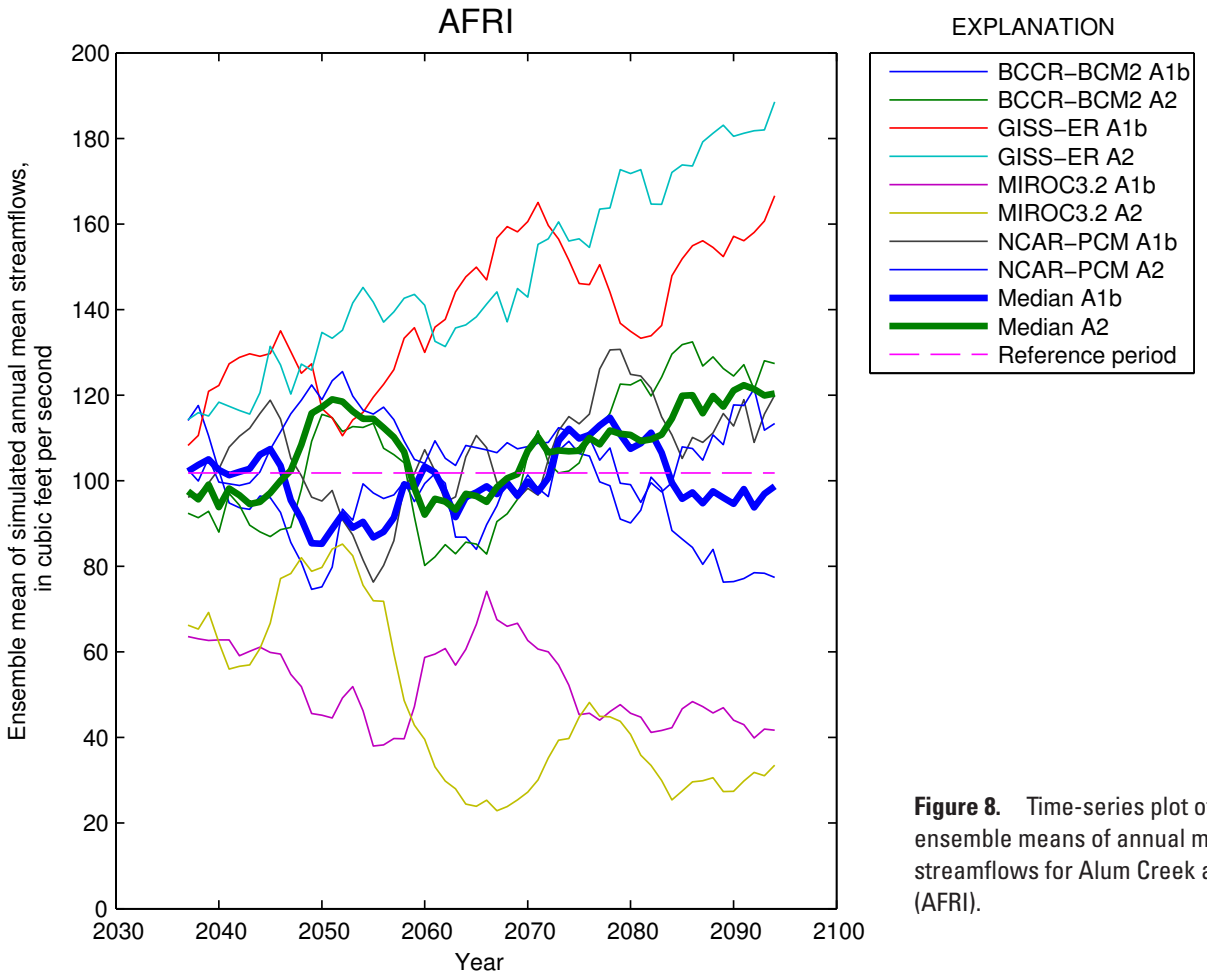

Figure 8. Time-series plot of level-1 ensemble means of annual mean streamflows for Alum Creek at Africa, Ohio (AFRI).

Similar to that done for annual means, for each model-output location, time series of ensemble means of monthly mean streamflows or water levels were computed for each level-1 GCM/emission-scenario output, and ensemble means based on 20 realizations were merged into one dataset so that each row of the dataset corresponded to a given month and year and each column corresponded to the ensemble means for one of the eight GCM/emission-scenario outputs. Medians of the ensemble means were computed for each month-year combination (each row) separately for model results based on the A1b and A2 emission scenarios, resulting in two new time series. The month- and emission-scenario-specific time series of the medians of the ensemble means each were divided into three "epochs" (where epoch 1 corresponds to dates between 2037 and 2055, epoch 2 corresponds to dates between 2056 and 2075, and epoch 3 corresponds to dates between 2076 and 2094) and notched boxplots were prepared (appendix C) showing the distribution of the medians within each epoch. Figure 9 shows an example of such a boxplot for the month of January for the model-output site at Alum Creek at Africa, Ohio (AFRI).

The boxplots are intended to aid in the identification of month-specific temporal trends in streamflows or water levels. As illustrated in figure 10, the top and bottom of the box represent the 75th and 25th percentiles of the distribution, respectively, the red line in the interior of the box is the 50th percentile (median), and the dashed vertical lines extend to the largest and smallest values that are within 1.5 times the interquartile range (IQR) (the distance between the 75th and 25th percentiles) from the top and bottom of the box. Values that are more than 1.5 times the IQR from the top or bottom of the box are considered outliers and are plotted with a red plus sign. The height of the notch (the portion of the box where the sides are angled) represents the 95-percent confidence interval for the median and is computed as 3.14 times the IQR divided by the square root of the number of observations for the epoch (Chambers and others, 1983). If the notches on two boxes do not overlap, then the medians of the two distributions are significantly different at about a 95-percent confidence level (assuming the datasets are independent and identically distributed random samples from two normally distributed populations). Sometimes (as shown in figure 9), a notch extends below or above the 25th or 75th percentile line, respectively. This results in a somewhat unusual looking boxplot, but otherwise the various elements of the boxplot retain their same meanings.

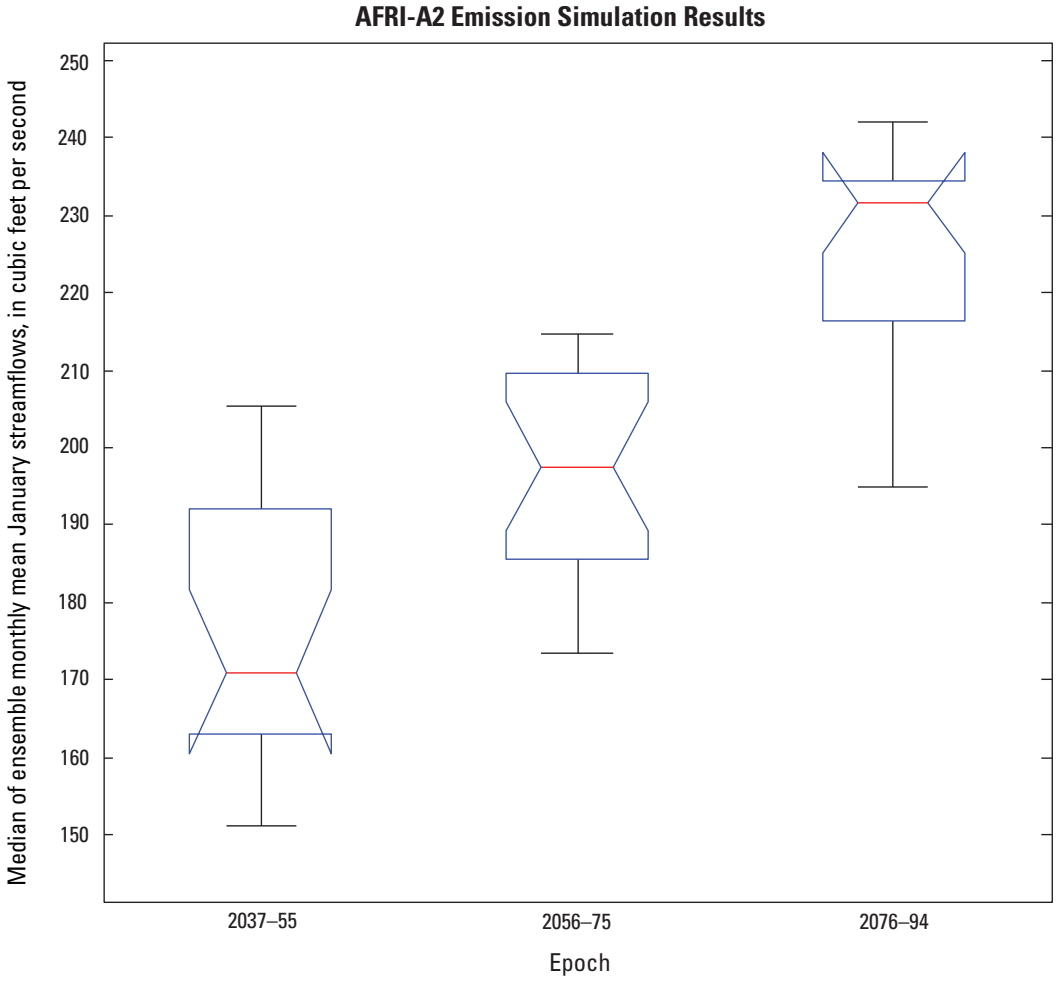

Figure 9. Example of notched boxplots showing the epoch-specific distributions of the level-1 medians of ensemble monthly mean January streamflows based on the A2 emission-scenario climate time series for Alum Creek at Africa, Ohio (AFRI).

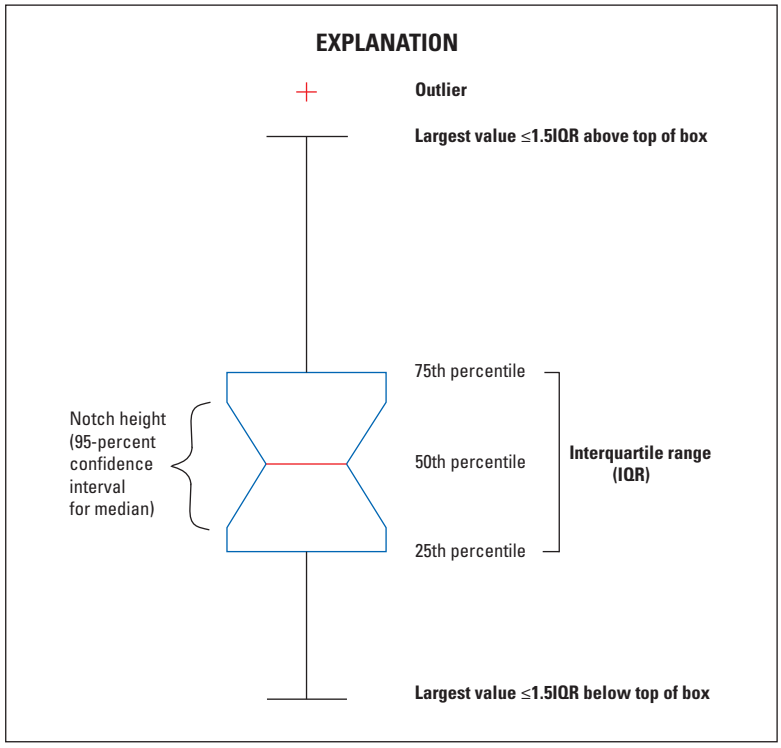

Figure 10. Explanation of boxplots.

Analysis of 7-, 30-, and 180-Day Average Streamflows and Reservoir Water Levels

Each of the level-1 simulations produced output time series of daily mean streamflows or water levels for periods of up to 22 years (the first 2 years of which were omitted from analyses). The daily simulation results were used to compute time series of running 7-, 30-, and 180-day averages, and then those running averages were analyzed to determine the minimum and maximum 7-, 30-, and 180-day average values associated with each simulation and model-output location. The minimum and maximum 7-, 30-, and 180-day averages for a given simulation were assigned a plotting year (that is, a year that the result is plotted at) approximately corresponding to the center of the simulation period. For example, a simulation beginning in 2016, which produced results through 2037, would provide usable data for the 20-year period 2018–2037 (after omitting the 2-year initialization period). In that case, the N-day (where N equals 7, 30, or 180) average minimum and maximum values for the simulation were assigned a plotting year of 2028 (the approximate center of the usable data period). Likewise, the N-day average minimum and maximum values for a simulation beginning in 2017, which produced results through 2038, provided usable data for the 20-year period 2019–2038 and was assigned a plotting year of 2029, and so forth. The datasets resulting from performing the analyses described above on each of the level-1 simulations for a given location consisted of annual time series of minimum and maximum N-day average values with each value in the time series representing the statistic for a specific simulation time period with a corresponding plotting year assigned as the approximate center of that time period. Statistics computed for time periods shorter than 20 years were omitted, resulting in final time series with (time-centered) plotting years ranging from 2028 to 2085.

The same analyses as those described above for the level-1 simulations also were done for the level-2 simulations; however, the minimum and maximum N-day moving averages were retained only for simulations whose time periods were centered within three specific 11-year periods: the target years of 2035, 2055, and 2075, plus and minus 5 years. For example, the 11-year period corresponding to the 2035 target year ranged from 2030 through 2040.

The level-2 simulation results can be viewed as reflecting the effects of anticipated changes in water use and land cover associated with development, combined with the changes in climate and operation of the upground reservoirs reflected in level-1 simulations. It is worth noting that the effects of development on hydrology at any given point in the study area are cumulative. For example, even though a particular subbasin might be expected to remain relatively unchanged with respect to its land-cover and (or) water-use characteristics at some future date, changes that occur in its upstream contributing drainage could result in appreciable change to the hydrology of that subbasin.

The level-1 and level-2 time series of time-centered minimum and maximum N-day average streamflows or water levels were separated into two sets: one set based on outputs for the A1b emission scenario and the second set based on outputs for the higher-emission A2 scenario. The median results for both emission scenarios (A1b and A2) were computed separately from the ensemble of simulation results for each plotting year and then the resulting time series were used to create a set of figures (appendix D). As illustrated in figure 11, lines and symbols colored red correspond to results based on climate scenarios derived from GCM outputs for the A1b emission scenario, and those colored blue correspond to the A2 emission-scenario-based results. The solid red and blue lines represent the medians of the level-1 simulation values, and the dashed red and blue lines represent the maximum and minimum values of the statistics in the level-1 simulation ensemble. The red and blue triangles represent the medians of the level-2 (development) simulation results for plotting years within the three 11-year periods associated with the target years. Although the level-2 results are plotted as individual symbols, each symbol represents the ensemble-median result for a given GCM/emission scenario, where each value in the ensemble represents the mean of 20 realizations of the statistic (each of which are themselves computed from 20 years of daily simulation results). Finally, the dashed horizontal magenta line corresponds to the value of the N-day statistic computed from simulation results for the reference period. The reference-period results are provided to permit comparisons with the level-1 and level-2 simulation results. To facilitate those comparisons, the reference-period line is shown as spanning the time period of the level-1 results even though the statistics for the reference period are based on simulation results for the period 1991–2010.

Seasonal analyses of minimum and maximum 7- and 30-day average streamflows and water levels from level-1 and level-2 simulations were done in a fashion analogous to that described above, the differences being that computations of the minimum and maximum 7- and 30-day average streamflows and water levels were based only on daily mean values occurring within the seasonal periods. The three "seasons" for which analyses were done consist of a "spring" season (defined as March through May), a "summer/fall" season (defined as June through October), and a "late-fall/winter" season (defined as November through February). Appendix E contains the results from the seasonal analyses. No seasonal analyses were done for 180-day average streamflows because the seasonal periods are shorter than 180 days. Seasonal analyses were done to provide more information on potential season-specific changes in streamflow and water-level conditions associated with climate change and development.

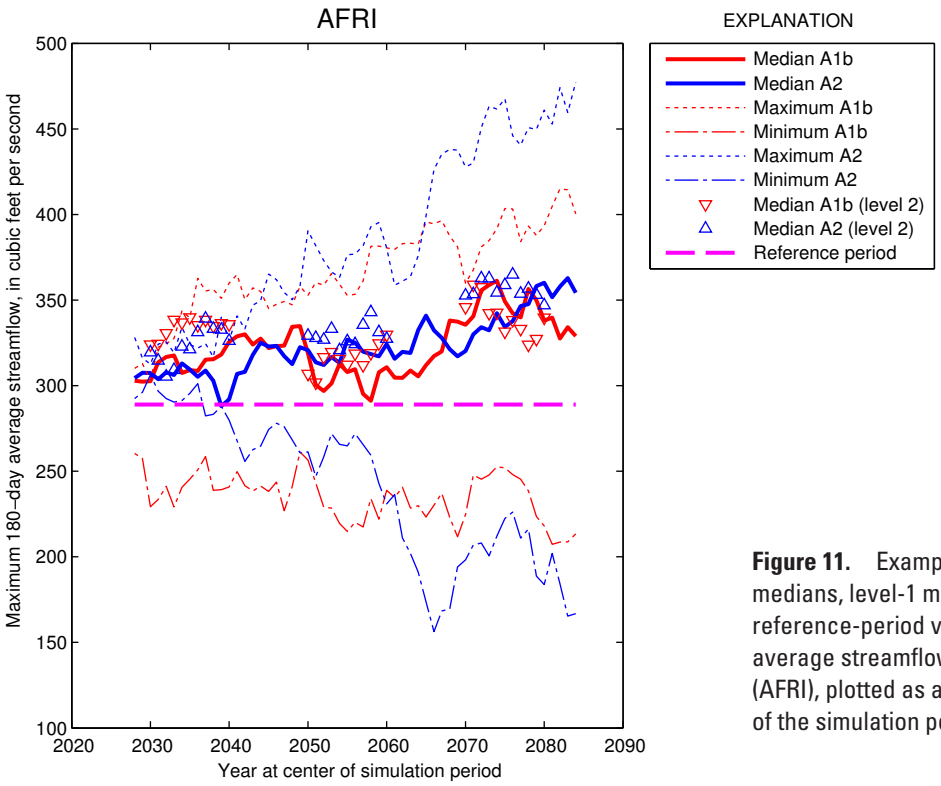

Figure 11. Example plot showing level-1 and level-2 medians, level-1 maximums and minimums, and the reference-period value of the maximum 180-day average streamflow at Alum Creek at Africa, Ohio (AFRI), plotted as a function of the year at the center of the simulation period.

Analysis of Duration Characteristics of 7- and 30-Day Running Average Streamflows and Reservoir Water Levels

Streamflow (or water-level) duration curves show the magnitudes of streamflows (or water levels) that are equaled or exceeded over a range of percentages of time during a particular time period. Duration curves (appendix F and appendix G) were prepared from time series of 7- and 30-day running average streamflows and water levels previously determined for the level-2 simulation results. For both the 7- and 30-day averaging periods, three figures were prepared for each location: one each based on times-series data for the 20-year period approximately centered on the target years of 2035, 2055, and 2075. Each figure shows the individual duration curves computed from level-2 results associated with each of the eight GCM/emission-scenario outputs. Each plot also shows a duration curve prepared from reference-period simulation results. The duration curves are intended to facilitate assessment of the variation in the quantiles of level-2 results for streamflow or water level for a given target year as a function of GCM/emission scenario and to facilitate comparisons between given target years.

Results and Discussion

The following discussions primarily address general trends observed for the various analyses of simulation results. Although it is beyond the scope of this study to address results in detail for each model-output location, selected results are discussed to illustrate potential uses and interpretations of the graph products provided in this report.

Annual Mean Streamflows and Reservoir Water Levels

Appendix B contains plots showing the ensemble means of level-1 simulated annual mean streamflows and water levels computed on the basis of the eight GCM/emission-scenario combinations. Also shown on the plots are median results for the A1b and A2 emission scenarios, as well as the mean annual streamflows or water levels computed from simulation results for the reference period.

In general, out of the eight GCM/emission-scenario combinations used in this study, model results based on the NASA/Goddard Institute for Space Studies GCM (GISS-ER) tended to show the highest annual mean streamflows and

water levels, and model results based on the GCM developed by the Center for Climate System Research National Institute for Environmental Studies and Frontier Research Center for Global Change (MIROC3.2) tended to show the lowest annual mean streamflows and water levels. This outcome is not surprising because the GISS-ER and MIROC3.2 GCMs ranked as showing the wettest and driest late 21st century conditions, respectively, of the GCMs used in this study.

Annual mean streamflow and water-level simulation results based on the GISS-ER and MIROC3.2 GCMs tended to diverge with time. Typically, late-21st-century annual mean streamflows differed by a factor of two to three from the lowest to the highest results. Compared to results based on the GISS-ER and MIROC3.2 GCMs, annual mean streamflow results based on the other two GCMs (BCCR-BCM2 and NCAR-PCM) tended to be more closely scattered around the reference-period means and did not exhibit as strong an indication of temporal trend.

The range in late 21st-century annual mean water-level results for the various GCM/emission-scenario outputs varied appreciably from reservoir to reservoir. Maximum absolute differences in late-21st-century annual mean water-level results ranged from as little as 0.9 to 1.1 feet for Griggs Reservoir to as much as 9.6 to 13.6 feet for Alum Creek Reservoir.

Similar to the simulation results based on the BCCR-BCM2 and NCAR-PCM GCMs, the medians of the A1b and A2 emission-scenario results tended to be relatively closely scattered around the reference-period means. Neither median result was consistently higher than the other over the entire simulation period. In most cases, the median A1b result was higher than the median A2 result until about 2047, and then the median A2 result was higher than the median A1b result until about 2059. From about 2059 to 2083, the median A1b and A2 results typically were similar in magnitude, and then the median A2 result typically was higher than the median A1b result from about 2083 to the end of the simulation period.

Indications of a possible late-21st-century temporal trend are stronger for results based on the A2 emission scenario as compared to results for the A1b emission scenario. Specifically, median streamflows and water levels for simulation results based on the A2 emission scenario tended to gradually (although not monotonically) increase after about 2059, with late-21st-century values ending higher than reference-period means. Conversely, median streamflows and water levels for simulation results based on the A1b emission scenario tended to increase from about 2059 to about 2073 and then leveled off or decreased, with late-21st-century values ending lower than reference-period means. The observed late-21st-century divergence in simulation results for these two emission scenarios may reflect the fact that the A1b emission scenario assumes that worldwide CO_2 emissions gradually decrease beginning around 2050, whereas CO_2 emissions continue to rise in the A2 emission scenario (fig. 2).

Monthly Mean Streamflows and Reservoir Water Levels

Notched boxplots (appendix C) were prepared that show the site-specific distribution of medians of the level-1 A2 and A1b emission-scenario ensemble monthly mean streamflows and water levels grouped into three epochs, where epoch 1 corresponds to dates between 2037 and 2055, epoch 2 corresponds to dates between 2056 and 2075, and epoch 3 corresponds to dates between 2076 and 2094. The epoch date ranges were chosen to divide the time period into approximately equal intervals of 19 to 20 years in length. The intent of the boxplots is to facilitate assessments of temporal trends in median simulated monthly mean streamflows and water levels and also provide information to permit assessment of distributional characteristics of simulated monthly mean streamflows and water levels as a function of time. Figure 12 summarizes the month-specific epoch-to-epoch directional changes in medians of the ensemble monthly mean streamflows and water-level results for the A2 and A1b emission scenarios. Solid filled arrows indicate that the epoch-to-epoch change was statistically significant (α=0.05). Note that not all the epoch-to-epoch changes shown in figure 12 were statistically significant.

An examination of boxplots for the median A2 emission-scenario results reveals several patterns:

- January mean streamflows or water levels increased from epochs 1 to 2, 2 to 3, and 1 to 3 at all sites. The increases from epochs 1 to 2 were statistically significant for about 75 percent of the sites, and 100 percent of the sites had statistically significant increases from epochs 2 to 3 and 1 to 3.

- February and March mean streamflows or water levels increased from epochs 2 to 3 and 1 to 3 at all sites. The February increases were statistically significant for more than 80 percent of the sites, and the March increases were statistically significant for 100 percent of the sites.

- April–November mean streamflows decreased from epochs 1 to 2 at all stream sites; however, with the exceptions of August and September, most of the stream sites also exhibited increases in mean streamflows between epochs 2 and 3. Ultimately, from epochs 1 to 3, 67 percent of the stream sites had statistically significant increases in June mean streamflows, and 100 percent of the stream sites had statistically significant decreases in August mean streamflows. All stream sites also exhibited decreases in September mean streamflows between epochs 1 and 3; however, the decreases were not statistically significant for most sites.

Site	Epoch	A2 emission scenario												A1b emission scenario											
		Month number												Month number											
		1	2	3	4	5	6	7	8	9	10	11	12	1	2	3	4	5	6	7	8	9	10	11	12
Stream sites																									
AFRI	1-2																								
	2-3																								
	1-3																								
CBUS	1-2																								
	2-3																								
	1-3																								
CCOL	1-2																								
	2-3																								
	1-3																								
CIRC	1-2																								
	2-3																								
	1-3																								
CLAR	1-2																								
	2-3																								
	1-3																								
DELA	1-2																								
	2-3																								
	1-3																								
LSCI	1-2																								
	2-3																								
	1-3																								
MILL	1-2																								
	2-3																								
	1-3																								
OLEN	1-2																								
	2-3																								
	1-3																								
OLOC	1-2																								
	2-3																								
	1-3																								
PROS	1-2																								
	2-3																								
	1-3																								
SROR	1-2																								
	2-3																								
	1-3																								
Lake/Reservoir sites																									
ALUM	1-2																								
	2-3																								
	1-3																								
DELL	1-2																								
	2-3																								
	1-3																								
GRIG	1-2																								
	2-3																								
	1-3																								
HOOV	1-2																								
	2-3																								
	1-3																								

Figure 12. Summary of month-specific epoch-to-epoch directional changes in medians of the level-1 A2 and A1b emission-scenario ensemble monthly mean streamflows and water levels (epoch 1 corresponds to dates from 2037 through 2055, epoch 2 corresponds to dates from 2056 through 2075, and epoch 3 corresponds to dates from 2076 through 2094; up arrow indicates an increase, down arrow indicates a decrease; solid-fill arrow indicates statistically significant change at α=0.05).

- Between epochs 1 and 3, all stream sites exhibited statistically significant increases in December mean streamflows.

- Results for reservoir sites were less consistent as a group than for stream sites, possibly reflecting the differing operational rules associated with each reservoir. That being said, between epochs 1 and 3, all reservoir sites exhibited increases in mean water levels for the months of January–April, June–July, and December, and all reservoir sites exhibited decreases in mean water levels for August. Many of the changes were not statistically significant; however, the increases for February were statistically significant for 80 percent of the reservoir sites, and the increases for January and March were statistically significant for 100 percent of the reservoir sites.

An examination of boxplots for the median A1b emission-scenario results also reveals several patterns:

- Increases or decreases in monthly mean flows or water levels that are consistent across all epoch comparisons (that is, epochs 1 and 2, 2 and 3, and 1 and 3) do not occur in results for the A1b scenario as they did with results for the A2 scenario and, for most comparisons, the percentage of sites exhibiting statistically significant increases or decreases in monthly mean streamflows or water levels is smaller in the A1b emission-scenario results than in the A2 emission-scenario results. Although the reason for this outcome is uncertain, it seems likely that, compared to the A2 emission scenario, the more favorable (lower) global CO_2 emission scenario reflected in the A1b emission-scenario results yielded climate changes that translated into more subtle changes in hydrology.

- When comparing results for epochs 1 and 3, there was a shift in the tendency for the A1b emission scenario results to show decreases or increases in certain monthly mean streamflows and water levels relative to the A2 results. In particular, decreases in streamflow or water level were more common in the A1b results than the A2 results for the months of February, June, July, and November, and increases were more common for September.

N-Day Average Streamflows and Reservoir Water Levels

To facilitate the subsequent discussions, N-day average streamflows or water levels hereafter will be referred to simply as N-day streamflows or water levels (for example, the minimum 7-day average streamflow will be referred to as the "minimum 7-day streamflow").

Appendix D contains plots showing the level-1 time series of time-centered minimum and maximum N-day streamflows or water levels (dashed narrow lines) separated into two groups: one group based on outputs for the A1b emission scenario and the second group based on outputs for the higher-emission A2 scenario. Also shown are the time series of median results for the level-1 (solid wide lines) and level-2 (triangles) A1b and A2 emission scenarios computed separately from the ensemble of simulation results for each plotting year. Wide dashed lines corresponding to the values of the N-day statistics computed from simulation results for the reference period are superimposed on the plots for reference.

In many of the plots, the spread between the maximum and minimum N-day streamflows or water levels widens as a function of time. This is particularly true for stream sites. Irrespective of the cause(s) for the widening, this suggests increasing uncertainty with time regarding magnitudes of the N-day flow statistics.

The wide dashed line representing the N-day statistic for the reference period typically lies mostly within the envelope formed by the lines representing the maximum and minimum values computed from the level-1 results. Even so, it is worth reiterating that simulation results for the reference period do not include effects of upground reservoirs (because the reservoirs had not been built) whereas, in addition to the effects of changes in climate, level-1 results do include effects of the upground reservoirs (as they are expected to come online).

The red and blue triangles represent the medians of level-2 A2 and A1b simulation results for plotting years within the three 11-year periods associated with the target years. The level-2 results reflect combined effects of upground-reservoir operations, changes in climate and land cover, and the cumulative impact of all withdrawals and return flows in the drainage down to and including the model-output location. Consequently, for example, if a model-output location is coincident with a point of withdrawal (such as for a water supply), the model results will reflect that withdrawal as well as any other modeled withdrawals and (or) return flows that occur in the drainage contributing to that point.

Similar to the results for the annual mean streamflows and water levels, neither curve representing A2 or A1b emission-scenarios results for the level-1 median N-day streamflow and water level statistics plotted consistently above nor below the other; however, directional biases relative to the reference-period statistic were more common. Those directional biases are characterized by having the level-1 median N-day streamflow or water-level results consistently plot above or below the line representing the reference-period statistic. Changes in climate and the addition of the upground reservoirs likely play a large role in those directional biases; however, calibration-related and time-sampling-related factors may also play a role.

At times, the triangles representing the level-2 medians of A2 and A1b simulation results plotted far away from the corresponding level-1 curve and, in some cases, a temporal

trend is evident. The reasons for those deviations and trends can be quite complex. For example, in the minimum 180-day water-level plot for Hoover Reservoir (HOOV, fig. 13), the level-2 medians gradually decrease over time, ending up more than 25 feet lower than the level-1 values. At the same time the minimum 180-day streamflows at CCOL (fig. 14) (about 0.4 mile downstream from the reservoir) increased, ending more than 33 percent (40 cubic feet per second [ft^3/s]) higher than level-1values. In this case, releases from Hoover Reservoir are modeled to change as a function of water demand at the Hap Cremean Water Treatment Plant (less than 5 miles downstream from the reservoir). As demand (based on projections) at the treatment plant increased over time, releases from the reservoir were increased to meet the demand (hence the increases at CCOL) and caused N-day minimum water levels in the reservoir to decrease. Level-2 minimum 180-day water levels also decreased over the same period in Alum Creek Reservoir (ALUM, fig. 15). The decrease in level-2 simulated water levels in Alum Creek Reservoir appears largely due to an operational rule (enforced in the model) that results in water being pumped from Alum Creek Reservoir to Hoover Reservoir when water levels in Hoover Reservoir are less than 889.23 feet (NGVD 29). Because of the increased demand at the Hap Cremean Water Treatment Plant, end-of-21st-century water levels in Hoover Reservoir generally were lower than 889.23 feet, resulting in nearly continuous transfer of water from Alum Creek Reservoir to Hoover Reservoir. In short, these results indicate that there may not be sufficient water to meet projected demand at the Hap Cremean Water Treatment Plant from Hoover and Alum Creek Reservoirs without severely lowering water levels in the two reservoirs. It is important to note that these predicted results are based on current reservoir operational rule sets and projected development. Changes to zoning, development plans, water distribution, or reservoir operations could occur in the future to lessen or eliminate the impacts on the reservoirs.

Another example of the level-2 values plotting far away from the corresponding level-1 curve can be observed in the minimum 180-day streamflow plot for MILL (fig. 16), about 1.5 miles upstream from the mouth of Mill Creek. The 2030 time-centered level-2 results start out more than 25 ft^3/s higher than the corresponding level-1 results, and the spread between the level-1 and level-2 results gradually increases to greater than 60 ft^3/s by 2085. This is a case where water demand by the City of Marysville is expected to increase by almost 250 percent between 2035 and 2090, with nearly equivalent increases in return flows. The City of Marysville obtains almost half its water from groundwater sources (table 4) and so for every unit volume of streamflow that is withdrawn and treated for use, nearly twice that volume is returned as treated wastewater. Consequently, the increase in demand results in a net increase in streamflow downstream from Marysville due to the augmentation from groundwater. Of course, the assumptions behind this result are that (1) there is no net consumption of water, (2) Marysville will continue to obtain 50 percent of its water from groundwater, and (3) that the withdrawal of groundwater, by itself, will not appreciably reduce streamflows. Similar results were observed for the Little Scioto River Basin (LSCI) because of projected changes in water use at the Aqua Ohio water-treatment facility that serves the City of Marion.

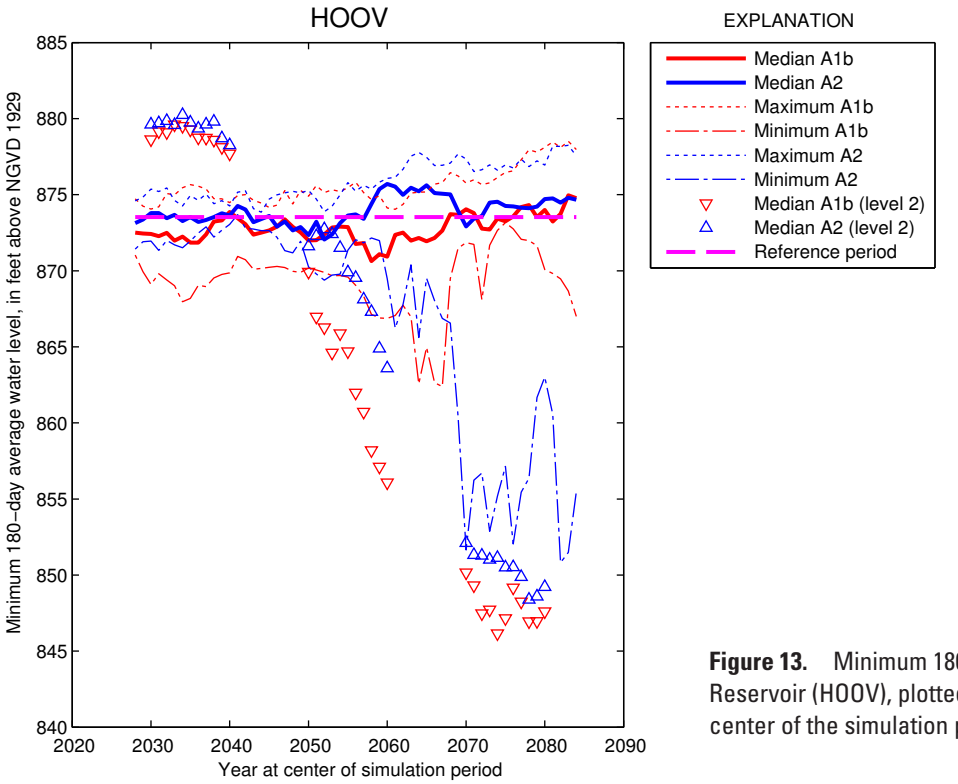

Figure 13. Minimum 180-day average water levels in Hoover Reservoir (HOOV), plotted as a function of the year at the center of the simulation period.

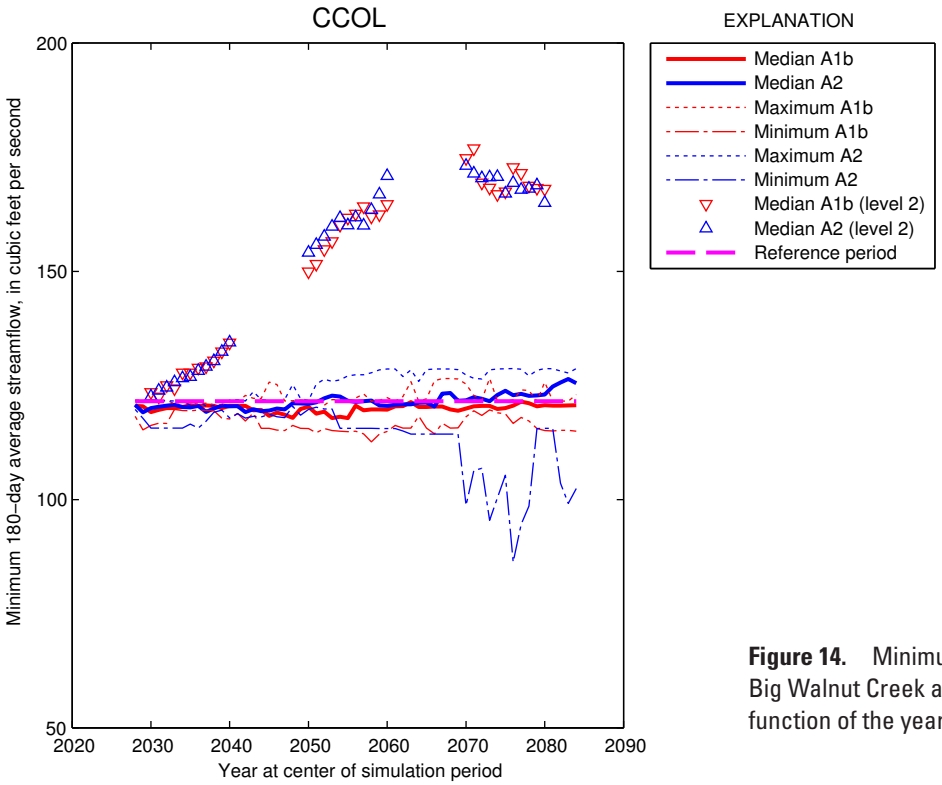

Figure 14. Minimum 180-day average streamflow at Big Walnut Creek at Central College (CCOL), plotted as a function of the year at the center of the simulation period.

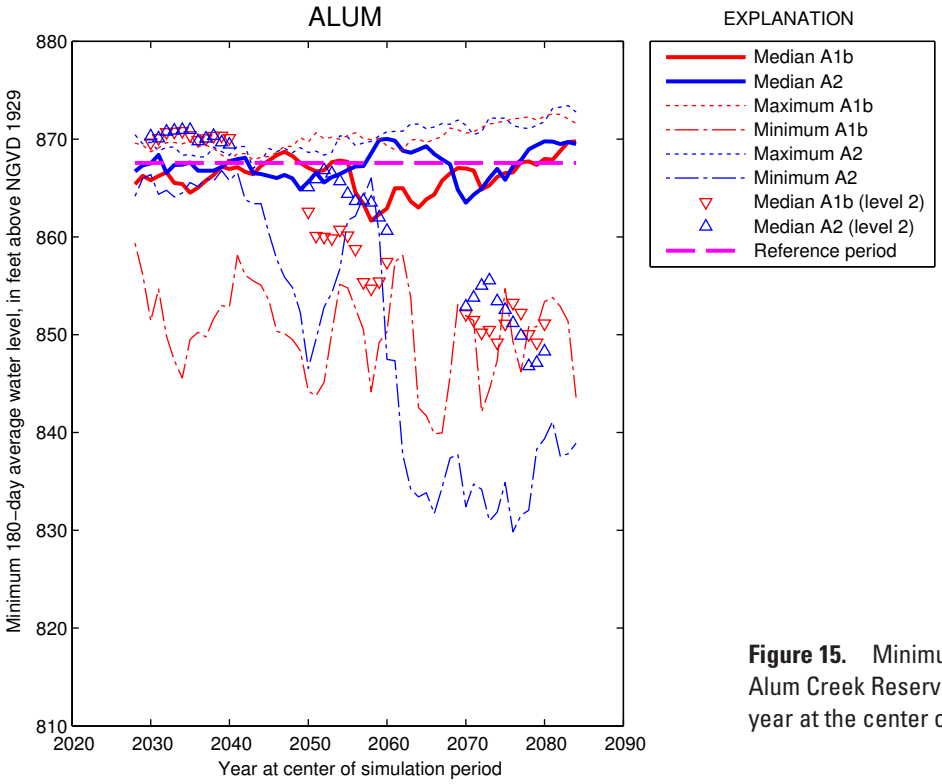

Figure 15. Minimum 180-day average water levels in Alum Creek Reservoir (ALUM), plotted as a function of the year at the center of the simulation period.

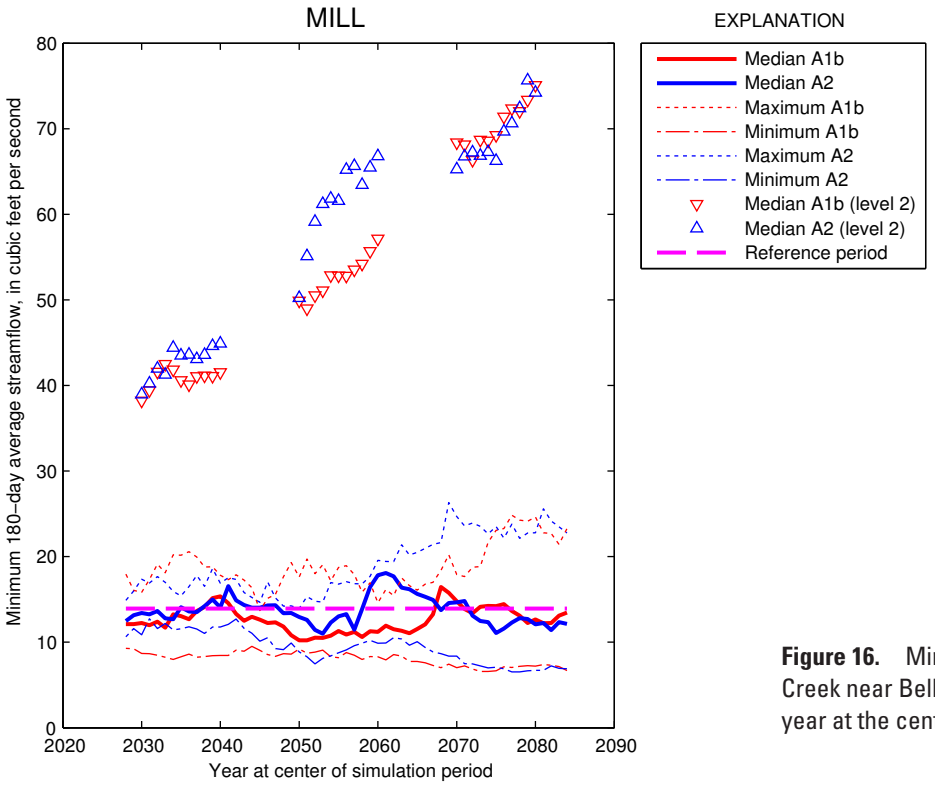

Figure 16. Minimum 180-day average streamflow at Mill Creek near Bellepoint (MILL), plotted as a function of the year at the center of the simulation period.

Appendix E contains plots that are identical in format to those in appendix D but separated into three seasonal periods: a "spring" season (defined as March through May), a "summer/fall" season (defined as June through October), and a "late-fall/winter" season (defined as November through February). As previously discussed, seasonal analyses of minimum and maximum 7- and 30-day streamflows and water levels from level-1 and level-2 simulations were based only on daily mean values occurring within the respective seasonal periods.

Seasonal analyses were done to provide information on season-specific changes in streamflow and water-level conditions associated with climate change and development. For example, an examination of the median level-1 A2 and A1b emission scenario results shown on the nonseasonal plot of minimum 30-day streamflows for OLOC (fig. 17) suggests that this statistic will decrease somewhat in the second half of the 21st century as compared to the first half of the 21st century. The level-2 results suggest that minimum 30-day streamflows will be appreciably lower than both the level-1 and reference-period results when development is considered in addition to climate change. An examination of the seasonal plots for OLOC (figs.18–20) provides more information on the seasonal character of the indicated changes. Specifically, the seasonal plots show that

1. the minimum 30-day streamflows that are reflected in nonseasonal plot (fig. 17) occurred during the summer/fall season,

2. the second-half-21st-century decreases in minimum 30-day streamflows observed with the nonseasonal median A2 and A1b level-1 results are not present in the plots for the spring season and are less apparent in plots for the late-fall/winter season,

3. level-2 minimum 30-day streamflows for the spring and late-fall/winter seasons typically were higher than those determined from level-1 results—only during the summer/fall season were level-2 results consistently (and appreciably) lower than the level-1 and reference-period results—and

4. beginning with simulation results centered on 2055, some level-2 minimum 30-day streamflows were zero, indicating that there may be periods in the summer/fall season when there is insufficient water available to meet the cumulative demands for water at OLOC (assuming current operational rules for Delaware Lake and anticipated changes in water use).

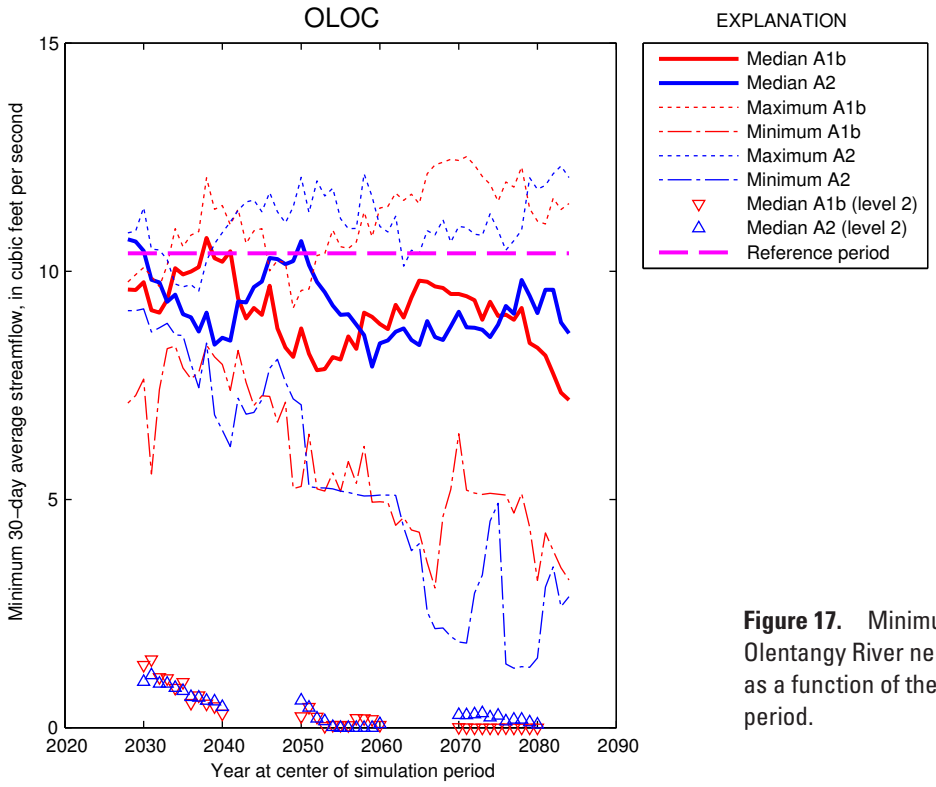

Figure 17. Minimum 30-day average streamflow at Olentangy River near Olentangy Caverns (OLOC), plotted as a function of the year at the center of the simulation period.

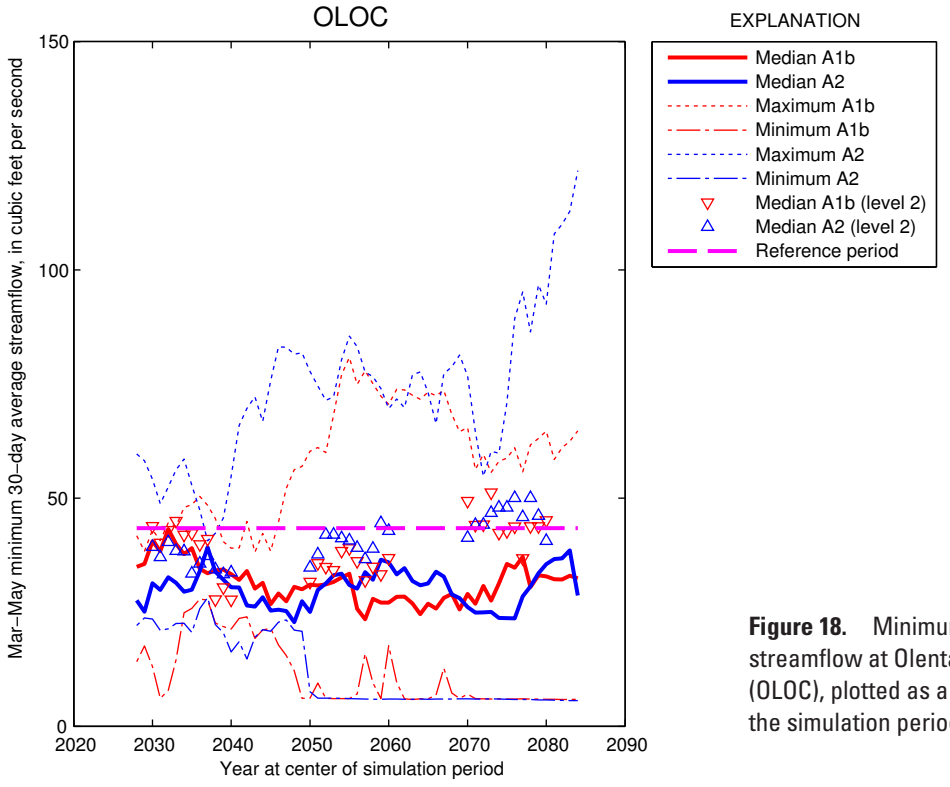

Figure 18. Minimum March–May 30-day average streamflow at Olentangy River near Olentangy Caverns (OLOC), plotted as a function of the year at the center of the simulation period.

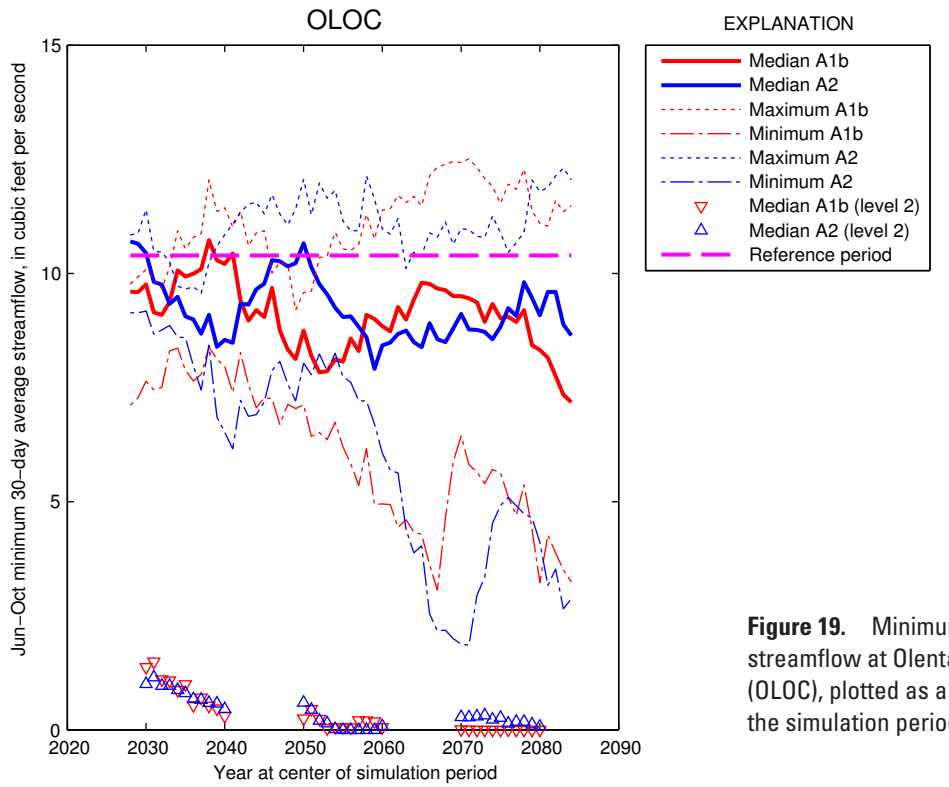

Figure 19. Minimum June–October 30-day average streamflow at Olentangy River near Olentangy Caverns (OLOC), plotted as a function of the year at the center of the simulation period.

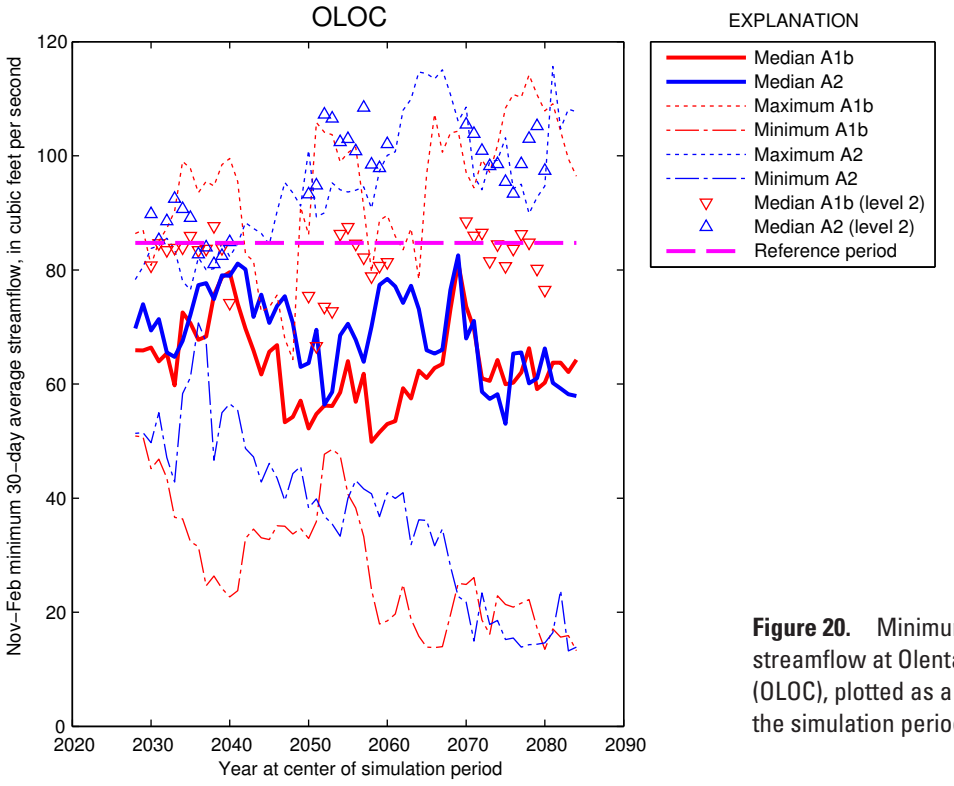

Figure 20. Minimum November–February 30-day average streamflow at Olentangy River near Olentangy Caverns (OLOC), plotted as a function of the year at the center of the simulation period.

It is worth reiterating that the level-2 N-day minimums (maximums) reflect the lowest (highest) N-day average streamflows or water levels that occurred during the 11-year period centered on the plotting year. Consequently, those values represent the extremes for those time periods and do not indicate how often those extremes occurred during the period. For example, if the minimum 7-day streamflow was determined to be 0.0 ft^3/s, the statistic provides no information regarding whether that minimum occurred only once or occurred frequently.

Duration Characteristics of 7- and 30-Day Running Average Streamflows and Reservoir Water Levels

Appendix F and appendix G contain duration plots prepared from time series of 7- and 30-day running average streamflows and water levels, respectively, determined from level-2 simulation results. Three plots are presented for each combination of averaging interval and output location. The three plots are based on level-2 times-series data for 20-year periods approximately centered on the target years of 2035, 2055, and 2075, respectively. For reference, a duration curve prepared from reference-period simulation results also is shown on each plot.

Duration plots were prepared to provide information on the distributional characteristics of simulated streamflows or water levels associated with each GCM/emission-scenario combination. For example the plots for CBUS (figs. 21–22) indicate that for the 20-year period centered on 2035, the median value (50th percentile) of the time series of 7-day average simulated streamflows for the eight GCM/emission-scenario combinations ranged from about 574 to 957 ft^3/s and, for the 20-year period centered on 2075, the median value ranged from about 377 to 1,250 ft^3/s. Consequently, when comparing the simulation results centered on 2075 relative to those centered on 2035, not only did the range in the median 7-day average streamflows for the eight GCM/emission-scenario combinations increase, but the low value was lower and the high value was higher. In addition, the ratio of the maximum to minimum values for the eight GCM/emission-scenario combinations for a given percentile was largest for the 50th percentile and then gradually decreased in magnitude towards both the higher and lower percentiles. This pattern suggests that the distributional changes between simulated streamflows for the various GCM/emission-scenario combinations tended to be smaller near the extremes of high and low flows than in the more central range of streamflows. Similar results were observed in duration plots for the 30-day streamflows (figs. 23–24); however, the largest maximum-to-minimum ratios were associated with the 60th or 70th percentiles of duration. Finally, at CBUS for both the 7-day and 30-day streamflows, the ordinates of the duration curve computed from simulation results for the reference period consistently fell within the bounds of the same-percentile ordinates of the maximum and minimum values computed from simulation results for the eight GCM/emission-scenario combinations. In other words, the duration curve for the reference period was enveloped by the level-2 duration curves for the eight GCM/emission-scenario combinations. This is true in spite of the fact that the level-2 results reflect changes in climate, land cover, and water use in addition to operation of the upground reservoirs, all of which are not reflected in the reference-period results. Consequently, if we consider the range of outcomes for the level-2 simulation results as an ad hoc measure of uncertainty, this suggests that we cannot be certain whether streamflows associated with any given flow quantile will increase or decrease in the future at this site.

The shape and character of duration curves for reservoir water levels was more variable than those for streamflows. In part, the greater variability is due to the differing operational rules at the reservoirs; however, between-reservoir differences in the relations between water level and reservoir volume also likely contribute to the observed variability. Similar to those for the streamflow sites, the ordinates of the duration curves for reservoirs computed from simulation results for the reference period consistently fell within the bounds of the same-percentile ordinates of the maximum and minimum values computed from simulation results for the eight GCM/emission-scenario combinations.

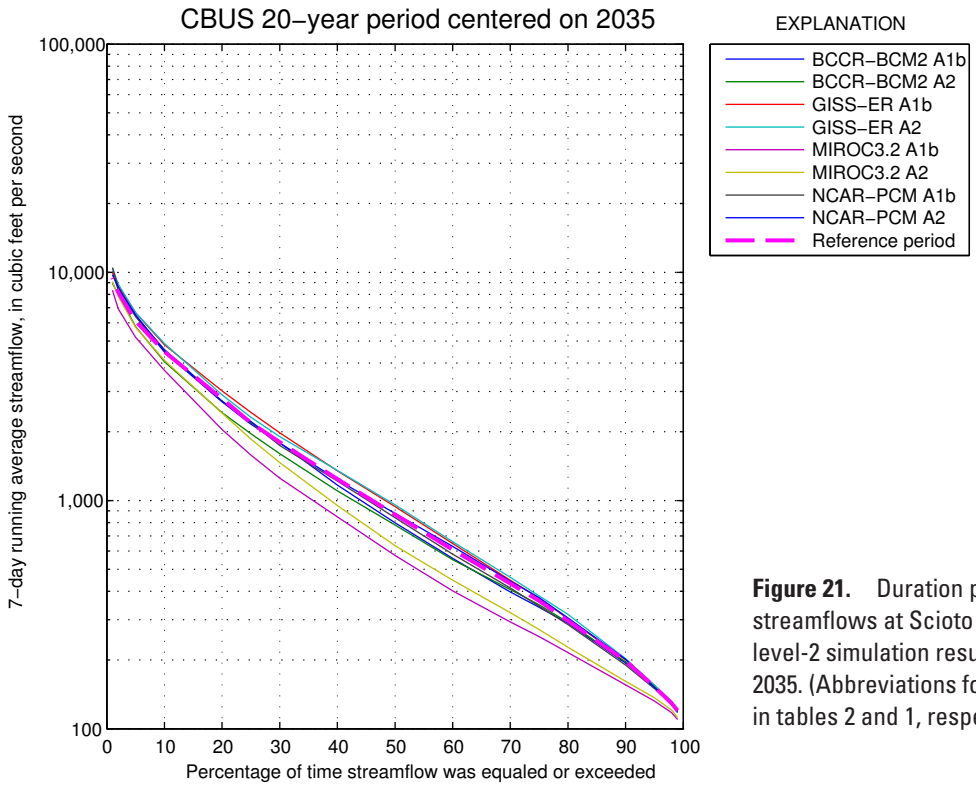

Figure 21. Duration plot of 7-day running average streamflows at Scioto River at Columbus (CBUS) based on level-2 simulation results for 20-year period centered on 2035. (Abbreviations for models and scenarios are defined in tables 2 and 1, respectively.)

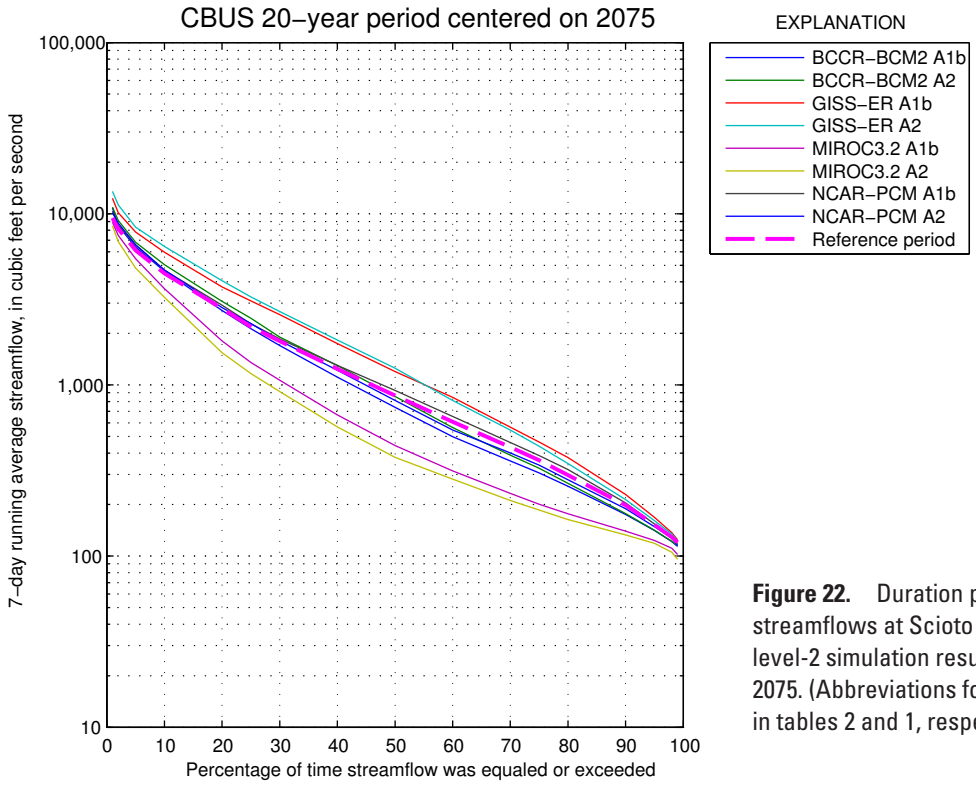

Figure 22. Duration plot of 7-day running average streamflows at Scioto River at Columbus (CBUS) based on level-2 simulation results for 20-year period centered on 2075. (Abbreviations for models and scenarios are defined in tables 2 and 1, respectively.)

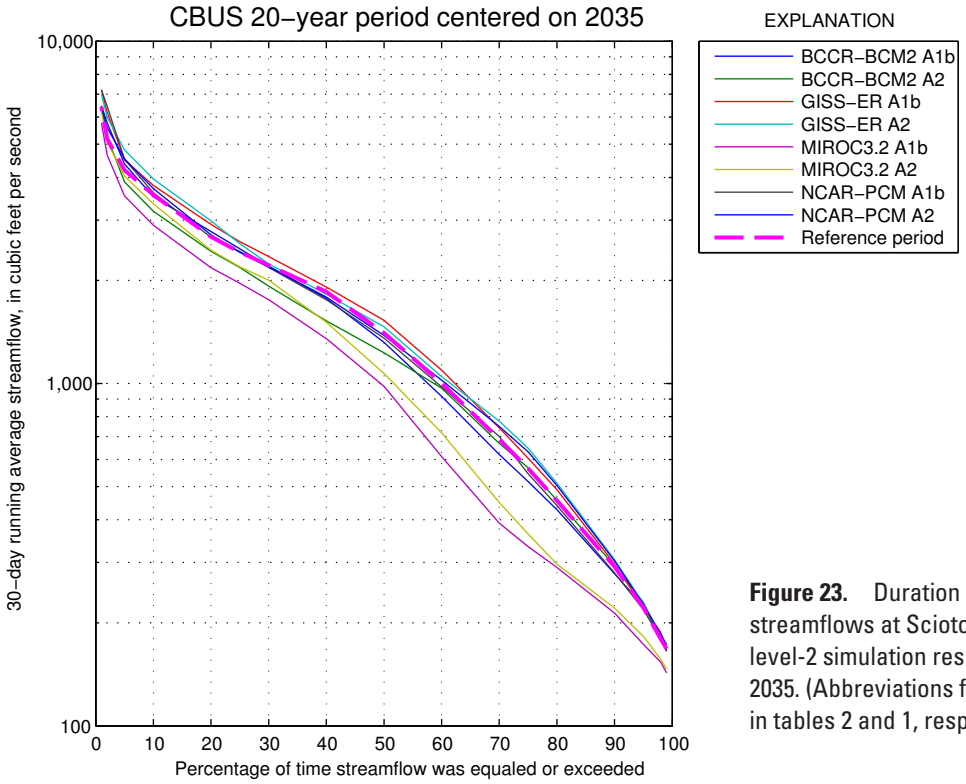

Figure 23. Duration plot of 30-day running average streamflows at Scioto River at Columbus (CBUS) based on level-2 simulation results for 20-year period centered on 2035. (Abbreviations for models and scenarios are defined in tables 2 and 1, respectively.

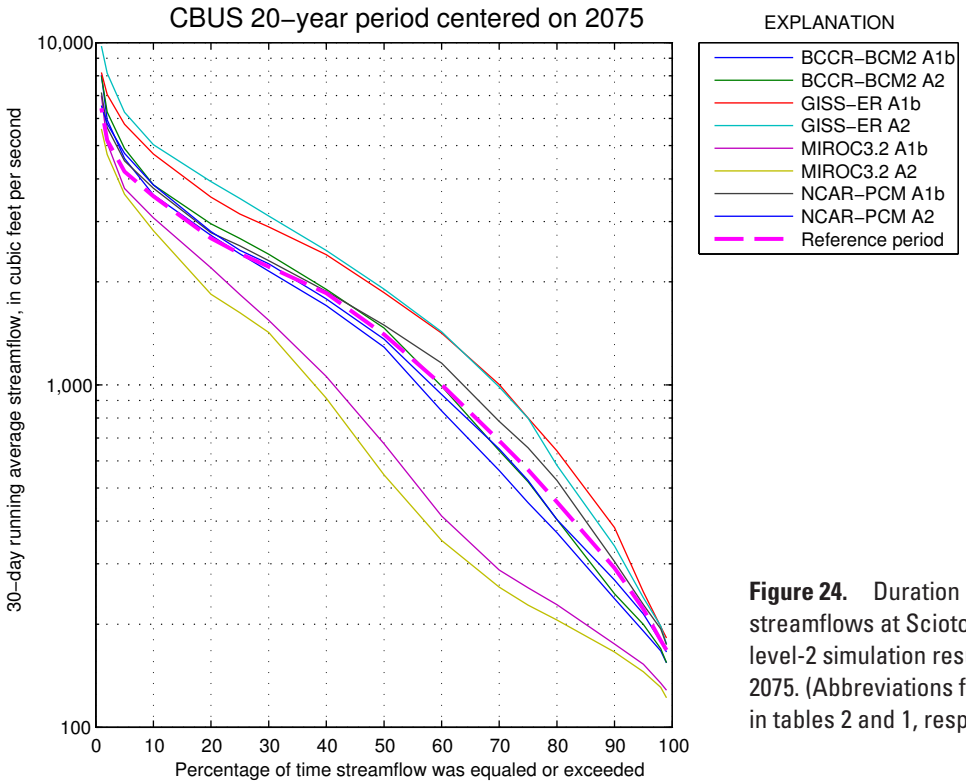

Figure 24. Duration plot of 30-day running average streamflows at Scioto River at Columbus (CBUS) based on level-2 simulation results for 20-year period centered on 2075. (Abbreviations for models and scenarios are defined in tables 2 and 1, respectively.)

Limitations

The results provided in this report are based on climate and hydrologic models that employ a number of assumptions and simplifications of complex real-world processes. Hence, there can be considerable uncertainty associated with some inputs to the models, and that uncertainty in inputs translates to uncertainty in results.

The historical climate records chosen to represent baseline conditions affect the precipitation-runoff modeling results because they served as a foundation on which the future climate time series were built. Although an attempt was made to select a historical time period that was reasonably representative with respects to trends, variability, and extremes in the longer climate record, it still represents an estimate of those characteristics.

Monthly change factors were applied to hourly historical climate data to estimate hourly future climate data. Although climate change may occur more gradually than implied by monthly change factors, the authors assumed that the amount of change that would occur over a 1-month period was not large enough to warrant the computation and application of change factors at time scales smaller than 1 month.

As previously mentioned, the monthly change-factor approach adopted for this study scales the historical climate record but does not alter its temporal sequence. So, if a GCM were to indicate short time-scale changes to durations of consecutive dry or wet days, those changes will not be reflected in the change-factor-adjusted climate (although their effects on monthly total precipitation, if any, will be represented). As a consequence, results derived for short averaging periods may be more subject to error than those derived for longer averaging periods. For this reason, as well as others, the model results are not suitable for addressing questions about instantaneous extremes such as annual peak flows.

The hydrologic models employ rule sets (algorithms) that govern the operation of the reservoirs. Although these rules are enforced in the model, in reality, the rules at times are treated by dam operators more like guidelines; that is to say, there have been times when the actual operation of the reservoirs deviates from the rule sets. Some reservoirs, such as O'Shaughnessy, historically have deviated from the rule sets more than others. The reasons for the deviations at O'Shaughnessy primarily are due to inconsistent operation of the hydraulic turbines, and the deviations represent a potential source of error and (or) uncertainty in model outcomes, particularly with respect to streamflow and water-level characteristics computed for short averaging periods.

Finally, model outputs associated with development conditions are based on estimates of future land cover and water demand. There could be appreciable changes in hydrology relative to that modeled should zoning, development plans, water distribution, and (or) reservoir operations change in a fashion different than expected.

References Cited

Bicknell, B.R., Imhoff, J.C., Kittle, J.L., Jr., Jobes, T.H., and Donigian, A.S., Jr., 2005, HSPF Version 12.2 user's manual: Mountain View, Calif., AQUA TERRA Consultants [variously paged].

Bureau of Reclamation, 2013, Downscaled CMIP3 and CMIP5 Climate and Hydrology Projections—Release of downscaled CMIP5 Climate Projections, comparison with preceding information, and summary of user needs: Denver, Colo., prepared by the U.S. Department of the Interior, Bureau of Reclamation, Technical Services Center, 47 p.

Chambers, J.M., Cleveland, W.S., Kleiner, B., and Tukey, P.A, 1983, Graphical methods for data analysis: Boston, Duxbury Press, Wadsworth Statistics/Probability Series, p. 62.

ClimateWizard, 2012, End-of-21st-century (2080s) departures in mean air temperature and precipitation for selected global climate models compared to the lowest and highest departures for the entire ensemble of models in Coupled Model Intercomparison Project phase 3 dataset: Map images generated from interactive database, accessed May 6, 2012, at http://www.climatewizard.org/.

Fowler, H.J., Blenkinsop, Stephen, and Tebaldi, Claudia, 2007, Review. Linking climate change modelling to impacts studies—Recent advances in downscaling techniques for hydrological modelling: International Journal of Climatology, v. 27, p. 1547–1578.

Fry, J., Xian, G., Jin, S., Dewitz, J., Homer, C., Yang, L., Barnes, C., Herold, N., and Wickham, J., 2011, Completion of the 2006 National Land Cover Database for the conterminous United States: Photogrammetric Engineering and Remote Sensing, v. 77, no. 9, p. 858–864.

Hay, L.E.; LaFontaine, Jacob; and Markstrom, S.L., 2014, Evaluation of statistically downscaled GCM output as input for hydrological and stream temperature simulation in the Apalachicola-Chattahoochee-Flint River Basin (1961–1999): Earth Interactions, v. 18, no. 9, p. 1–32

Hay, L.E., and McCabe, G.J., 2010, Hydrologic effects of climate change in the Yukon River Basin: Climatic Change, v. 100, p. 509–523.

Intergovernmental Panel on Climate Change (IPCC), 2000, Special Report on Emissions Scenarios—A special report of Working Group III of the Intergovernmental Panel on Climate Change [Nakicenovic, Nebojsa, and Swart, Rob, eds.]: Cambridge and New York, Cambridge University Press, accessed April 23, 2014, at http://www.grida.no/climate/ipcc/emission/index.htm.

Intergovernmental Panel on Climate Change (IPCC), 2014, Summary for policymakers, in Climate Change 2014, Mitigation of Climate Change—Contribution of Working Group III to the Fifth Assessment Report of the Intergovernmental Panel on Climate Change [Edenhofer, O., Pichs-Madruga, R., Sokona, Y., Farahani, E., Kadner, S., Seyboth, K., Adler, A., Baum, I., Brunner, S., Eickemeier, P., Kriemann, B., Savolainen, J., Schlömer, S., von Stechow, C., Zwickel, T., and Minx, J.C., eds.]: Cambridge and New York, Cambridge University Press.

Markstrom, S.L., Hay, L.E., Ward-Garrison, C.D., Risley, J.C., Battaglin, W.A., Bjerklie, D.M., Chase, K.J., Christiansen, D.E., Dudley, R.W., Hunt, R.J., Koczot, K.M., Mastin, M.C., Regan, R.S., Viger, R.J., Vining, K.C., and Walker, J.F., 2012, Integrated watershed-scale response to climate change for selected basins across the United States: U.S. Geological Survey Scientific Investigations Report 2011–5077, 143 p.

Meehl, G.A., Covey, C., Delworth, T., Latif, M., McAvaney, B., Mitchell, J.F.B., Stouffer, R.J., and Taylor, K.E., 2007, The WCRP CMIP3 multimodel dataset—A new era in climate change research: Bulletin of the American Meteorological Society, v. 88, p. 1383–1394.

National Oceanic and Atmospheric Administration, 2014, Climate at a glance: National Climatic Data Center, accessed May 6, 2014, at http://www.ncdc.noaa.gov/cag/.

Ohio Division of Geological Survey, 1998, Physiographic regions of Ohio: Ohio Department of Natural Resources, Division of Geological Survey, page-size map with text, 1 p., scale 1:2,000,000.

Ohio Division of Geological Survey, 2006, Geologic map and cross section of Ohio: Ohio Department of Natural Resources, Division of Geological Survey, page-size map with text, 2 p., scale 1:2,100,000.

SAS Institute, Inc., 2014a, Base SAS® 9.3 procedures guide—Statistical procedures. The UNIVARIATE procedure—Calculating percentiles: Accessed June 25, 2014, at http://support.sas.com/documentation/cdl/en/procstat/63963/HTML/default/viewer.htm#univariate_toc.htm.

SAS Institute, Inc., 2014b, SAS/ETS® user's guide—Procedure reference. The EXPAND procedure: Accessed June 25, 2014, at http://support.sas.com/documentation/cdl/en/etsug/60372/HTML/default/viewer.htm#expand_toc.htm.

Schiefer, M.C., 2002, Basin descriptions and flow characteristics of Ohio streams: Ohio Department of Natural Resources, Division of Water, Bulletin 47, 161 p.

U.S. Census Bureau, 2014, Interactive population map: Accessed May 5, 2014, at http://www.census.gov/2010census/popmap.

Vogel, R.M., and Fennessey, N.M., 1994, Flow-duration curves. I—New interpretation and confidence intervals: Journal of Water Resources Plannning and Management, v. 120, no. 4, p. 485–504.

Publication services provided by the U.S. Geological Survey
Science Publishing Network
Columbus Publishing Service Center

For more information concerning the research in this report contact the

Director, Ohio Water Science Center

6480 Doubletree Ave

Columbus, OH 43229-1111

http://oh.water.usgs.gov/

ISSN 2328-0328 (online)
http://dx.doi.org/10.3133/sir20155024